# Olfactory Pathway of the Hornet *Vespa velutina*: New Insights Into the Evolution of the Hymenopteran Antennal Lobe

Antoine Couto,[1] Benoit Lapeyre,[1] Denis Thiéry,[2,3] and Jean-Christophe Sandoz[1]*

[1]Laboratory Evolution Genome Behavior and Ecology, CNRS, Université Paris-Sud, IRD, Université Paris Saclay, F-91198, Gif-sur-Yvette, France
[2]UMR 1065 Santé et Agroécologie du Vignoble, INRA, F-33883, Villenave d'Ornon, France
[3]Université de Bordeaux, ISVV, UMR 1065 Santé et Agroécologie du Vignoble, Bordeaux Sciences Agro, F-33883, Villenave d'Ornon, France

## ABSTRACT

In the course of evolution, eusociality has appeared several times independently in Hymenoptera, within different families such as Apidae (bees), Formicidae (ants), and Vespidae (wasps and hornets), among others. The complex social organization of eusocial Hymenoptera relies on sophisticated olfactory communication systems. Whereas the olfactory systems of several bee and ant species have been well characterized, very little information is as yet available in Vespidae, although this family represents a highly successful insect group, displaying a wide range of life styles from solitary to eusocial. Using fluorescent labeling, confocal microscopy, and 3D reconstructions, we investigated the organization of the olfactory pathway in queens, workers, and males of the eusocial hornet *Vespa velutina*. First, we found that caste and sex dimorphism is weakly pronounced in hornets, with regard to both whole-brain morphology and antennal lobe organization, although several male-specific macroglomeruli are present. The *V. velutina* antennal lobe contains approximately 265 glomeruli (in females), grouped in nine conspicuous clusters formed by afferent tract subdivisions. As in bees and ants, hornets display a dual olfactory pathway, with two major efferent tracts, the medial and the lateral antennal lobe tracts (m- and l-ALT), separately arborizing two antennal lobe hemilobes and projecting to partially different regions of higher order olfactory centers. Finally, we found remarkable anatomical similarities in the glomerular cluster organizations among hornets, ants, and bees, suggesting the possible existence of homologies in the olfactory pathways of these eusocial Hymenoptera. We propose a common framework for describing AL compartmentalization across Hymenoptera and discuss possible evolutionary scenarios. J. Comp. Neurol. 524:2335–2359, 2016.



**INDEXING TERMS:** social insects; wasps; three-dimensional reconstruction; macroglomerulus; RRID:SCR_000450; RRID:SCR_003070; RRID:SCR_007353; RRID:SCR_013672

Insects are influential models in the study of the evolution of olfactory processing and have revealed how selection pressures influence the organization and complexity of the olfactory system (Rospars, 1988; Kleineidam and Rössler, 2009; Ramdya and Benton, 2010; Hansson and Stensmyr, 2011). In insects, volatile molecules are detected by olfactory sensory neurons (OSNs) housed in cuticular sensilla on the antennae (Zacharuk, 1980). These neurons project to a primary olfactory center, the antennal lobe (AL), where they synapse onto local interneurons and projection neurons (PNs), within dense syn-



Additional Supporting Information may be found in the online version of this article at Wiley Online Library.

Grant sponsor: Région Ile-de-France; Grant number: DIM R2DS, project 2011-05 (to J.C.S.).

*CORRESPONDENCE TO: J.C.S. Sandoz, Laboratory Evolution Genome Behavior and Ecology, CNRS, Université Paris-Sud, IRD, Université Paris Saclay, 1 avenue de la Terrasse, F-91198 Gif-sur-Yvette, France. E-mail: sandoz@egce.cnrs-gif.fr

This article was published online on 07 March 2016. An error was subsequently identified. This notice is included in the online versions to indicate that have been corrected 28 March 2016.

Received November 20, 2015; Revised January 20, 2016;
Accepted January 29, 2016.
DOI 10.1002/cne.23975
Published online March 7, 2016 in Wiley Online Library (wileyonlinelibrary.com)

aptic neuropils, the glomeruli (Hildebrand and Shepherd, 1997; Anton and Homberg, 1999; Vosshall et al., 2000). PNs convey the olfactory message processed within AL networks to higher order olfactory centers, the mushroom body (MB) and/or the lateral horn (LH).

Many previous works have revealed specific adaptations in AL organization, in relation to the particular biology and ecology of a wide range of insect species (Rospars, 1983; Martin et al., 2011; Clifford and Riffell, 2013). For instance, whereas the number of AL glomeruli is almost invariant among individuals of a given species, it varies greatly between species, which is thought to be related to the complexity of their olfactory environments (Anton and Homberg, 1999; Hansson and Anton, 2000; Kelber et al., 2009). Another striking example of such neuroanatomical and physiological adaptations is the existence of enlarged glomeruli, called *macroglomeruli*, dedicated to pheromone detection and processing (Burrows et al., 1982; Arnold et al., 1985; Hanson et al., 1992; Sandoz, 2006; Nishikawa et al., 2008; Nishino et al., 2012). In most cases, macroglomeruli are male dimorphic adaptations devoted to sex pheromone processing, but they have also been discovered in the females of some social Hymenoptera (Arnold et al., 1988; Kleineidam et al., 2005; Roselino et al., 2015). In leaf-cutting ants, for instance, a macroglomerulus found only in large workers is thought to process trail pheromone information (Kelber et al., 2009; Kuebler et al., 2010). Thus, the presence of hypertrophied glomeruli may inform about particular pheromonal communication channels in a species.

In some cases, neuronal adaptations of the olfactory pathway are found throughout a specific taxon. For instance, in Hymenoptera, uniglomerular PNs project to the MB and the LH through two parallel output tracts, the medial and the lateral antennal lobe tracts (m- and l-ALT). The AL is thus composed of two hemilobes which send their information separately to both higher order centers (Abel et al., 2001; Galizia and Rössler, 2010; Rössler and Zube, 2011; Rössler and Brill, 2013). Investigations in basal Hymenoptera showed that this neuronal organization is present in some sawfly (Symphyta) families but absent in others, leading to the hypothesis that it has evolved in basal Hymenoptera (Dacks and Nighorn, 2011; Rössler and Zube, 2011). The benefit of this parallel processing system and the selective pressures that favored its evolution remain unknown. Some authors hypothesized that it could represent a preadaptation to high demands on olfactory discrimination needed for particular life styles such as parasitism, central place foraging, or sociality (Galizia and Rössler, 2010; Rössler and Zube, 2011). These examples demonstrate that essential knowledge on the evolution of the insect olfactory system can be obtained from its comparative analysis in well-chosen taxa. Thus, comparing the organization of the AL and its specific adaptations in terms of glomerular number, size, and input–output connectivity may allow one to understand adaptations linked to changes in diet, host preference, or social life style in Hymenoptera (Rospars, 1983; Zube and Rössler, 2008; Kelber et al., 2009; Dacks et al., 2010; Ibba et al., 2010; Das and Fadamiro, 2013; Guidobaldi et al., 2014).

Social insects ensure colony defense and cohesion, division of labor, and behavioral regulation through a highly elaborate communication system (Vander Meer, 1998). Specific adaptations of the olfactory pathway can be observed among the different members of a eusocial insect colony, which are usually revealed through sex and caste polymorphism (Zube and Rössler, 2008; Groh and Rössler, 2008; Kuebler et al., 2010; Nakanishi et al., 2010; Stieb et al., 2011; Roselino et al., 2015). Eusociality has appeared several times in Hymenoptera, in at least three different families, Apidae (bees), Formicidae (ants), and Vespidae (wasps and hornets; Hines et al., 2007; Hughes et al., 2008; Cardinal and Danforth, 2011; Johnson et al.; 2013). Although possible adaptations of olfactory circuits related to the social life style have been investigated in several Apidae (honeybees, stingless bees; Arnold et al., 1985; Flanagan and Mercer, 1989; Galizia et al., 1999; Kelber et al., 2006; Nishino et al., 2009; Streinzer et al., 2013; Roselino et al., 2015) and Formicidae (several ant species; Nishikawa et al., 2008; Zube and Rössler, 2008; Mysore et al., 2009; Nakanishi et al., 2010; Stieb et al., 2011; Kuebler et al., 2010), Vespidae are poorly documented. This group, however, is a key group for studying the evolution of eusociality because it contains species with a wide range of social organizations, from solitary to eusocial (Hunt, 2007; Pickett and Carpenter, 2010).

In their highest level of sociality, Vespidae display a large repertoire of odor-guided behaviors, comparable to those of ants and bees, including kin recognition and cooperation for brood care, colony defense, and foraging (Spradbery, 1973; Edwards, 1980; Matsuura and Yamane, 1990; Oi et al., 2015). Hornets (*Vespa* sp.) are the largest eusocial wasps. They are generalist foragers that gather carbohydrates and proteins for their progeny, by exploiting flower nectar, tree sap, fruit pulp, and arthropod prey (Raver et Richter, 2000). For such task, they use odors emanating from the food sources but also intraspecific olfactory recruitment signals, which increase their foraging efficiency (Ono et al., 1995, 2003; Brodmann et al., 2009; Couto et al., 2014). Females can release scent marks that are used by both workers and males to locate the nest (Batra,

1980; Steinmetz et al., 2002; Tan, 2014). Within the nest, hornets live in organized colonies with a highly efficient task allocation system regulated through social pheromones acting on workers (Ikan et al., 1969; Ishay, 1973; Veith et al., 1984; Monceau et al., 2013). To prevent exploitation of such altruistic behavior by alien individuals, hornets are also able to discriminate nestmates and nonnestmates by means of cuticular hydrocarbons (Ruther et al., 1998; Ruther et al., 2002). In addition, queens produce a sex pheromone that triggers copulatory behavior in males (Batra, 1980; Ono and Sasaki, 1987; Spiewok et al., 2006). Therefore, both hornet males and females develop and live in a rich olfactory environment and use a wide range of inter- and intraspecific chemical cues (Bruchini et al., 2010).

To date very few works have described the central nervous system of Vespidae, and most studies date back more than a century (Flögel, 1878; Viallanes, 1887; Von Alten, 1910). Flögel (1878) proposed the first anatomical description of the wasp brain and observed striking differences in the morphology of its MBs compared with the brains of other eusocial Hymenoptera, such as ants and honeybees. This was confirmed by Viallanes (1887), who reported that despite the huge size of their MBs, the vertical ($\alpha$) and medial ($\beta$) lobes appear atrophied. More recently, Ehmer and Hoy (2000) highlighted a strong anatomical divergence of MBs within this family, which could, however, not be related to the social organization level of the investigated species. Since then, neuroanatomical studies on the wasp or hornet brain have focused mainly on higher order centers (O'Donnell et al., 2004, 2011, 2015), but its olfactory pathway, and especially the AL, which may support important adaptations for foraging, pheromonal processing, and/or sociality, has been the subject of little consideration. According to Hanström (1928), the AL of social wasps would contain $\sim$1,000 small glomeruli arranged in multiglomerular layers, as in locusts (Hansson and Anton, 2000). In theory, such a high number of glomeruli would be consistent with the rich olfactory environment of these species. However, in light of recent data, serious doubts can be raised concerning Hanström's (1928) description (Kelber et al., 2009). First, none of the Hymenoptera studied so far displays such a high number of glomeruli, the maximum being 630 glomeruli in the ant *Apterostigma* cf. *mayri* (Kelber et al., 2009). Second, given current knowledge on the neural organization of the olfactory pathways of the different insect orders, it seems highly unlikely that the hornet AL presents a true locust-like organization, especially with regard to PN arborization. Whereas PNs are multiglomerular in locusts (Ignell, 2001; Ignell et al., 2001; Anton et al., 2002), Hymenoptera typically display two major tracts of uniglomerular PNs and three lesser tracts of multiglomerular PNs, which form a broad network in the protocerebrum (mediolateral ALT, ml-ALT; Abel et al., 2001; Kirschner et al., 2006; Galizia and Rössler, 2010; Rössler and Zube, 2011).

We performed a detailed neuroanatomical exploration of the olfactory pathway of a eusocial member of the Vespidae, the hornet *Vespa velutina*. This otherwise typical hornet species is particularly remarkable for its ecological success when introduced to new locations, such as in Europe, in which it has become an invasive species (Monceau et al., 2014; Arca et al., 2015). A nest founded by a single mated queen can produce up to 13,000 individuals, mostly sterile females (workers), which actively cooperate for the survival of the colony (Rome et al., 2015). They are vigorous predators of insects and very actively prey on honeybees, representing a threat for both local biodiversity and beekeeping activities (Monceau et al., 2014). Using fluorescent dye injection coupled with confocal microscopy, we compared AL features in queens, workers, and males. We asked whether the hornet olfactory system displays caste- or sex-specific adaptations, potentially related to the roles of the different members of a hornet colony. In particular, we looked for differences in the organization, size, and volume of AL glomeruli. Furthermore, from an evolutionary perspective, we investigated the input–output connectivity of the AL and compared it with the well-described olfactory pathways of ants and honeybees.

## MATERIALS AND METHODS

### Animals

Queens, workers, and males of the yellow-legged hornet, *Vespa velutina,* were used in the experiments. Queens and workers were obtained from field trapping in the area of INRA-Bordeaux Aquitaine (France) between April and November. Males were collected from wild nests in September in the same area. Males were identified by their specific morphological features such as long antennae (11 antennal segments instead of 10 in females) and the lack of a sting. Females were assigned to the reproductive or sterile caste by measuring their wing area according to Perrard et al. (2012). Wings were carefully flattened and clamped between two glass slides before capturing images with a film scanner (OpticFilm 7400, Plustek, Taipei, Taiwan). Wing size was evaluated in ImageJ (RRID:SCR_003070). A proxy measure of wing size was defined as the area between nine conspicuous vein intersections of the forewing (Fig. 1A, corresponding to landmarks 1–4, 9, 10, 13, 15, and 16 of Perrard et al., 2012). In hornets, queens are usually larger than workers

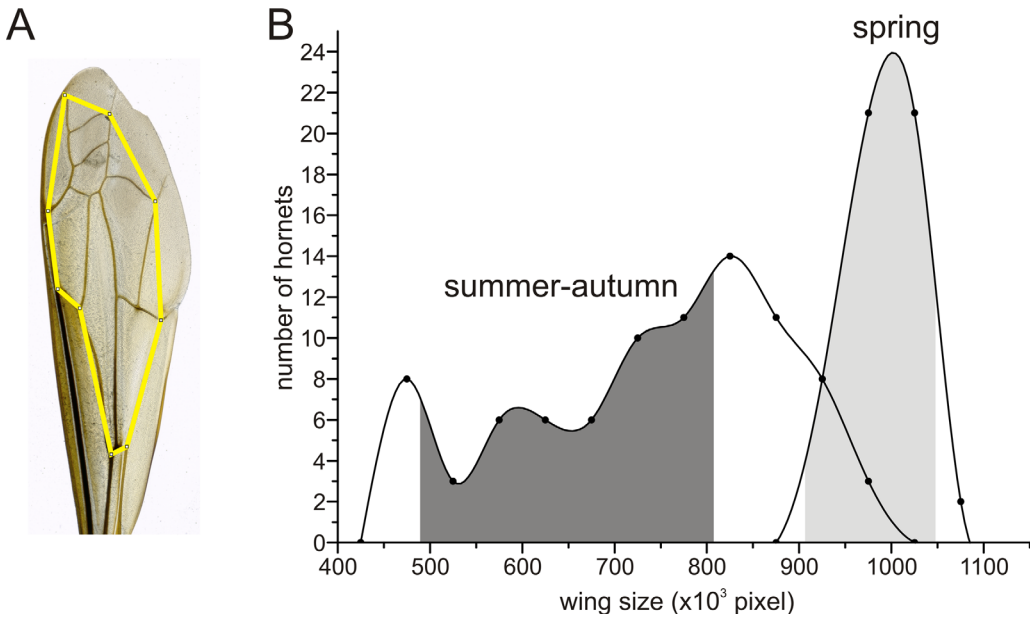


**Figure 1.** Wing size in *V. velutina* females. **A:** The area between nine vein intersections on the forewing (yellow polygon) was calculated as a proxy of wing size. **B:** Distribution of the wing sizes of all *V. velutina* females caught. Females caught in spring (April–May), at the start of the season, are necessarily founding queens. Females caught in summer–autumn (June–November) are mostly workers. Initially, workers are much smaller than queens. However, worker wing size increases throughout the colony cycle and may eventually (at the end of autumn) overlap with that of queens. Therefore, small individuals caught during summer and autumn (dark gray area) and large individuals trapped in spring (light gray area), which could be unambiguously assigned to workers and queens, respectively, were used in the experiments. [Color figure can be viewed in the online issue, which is available at wileyonlinelibrary.com.]

(Matsuura and Yamane, 1990). However, in *V. velutina*, this difference is not so clear-cut as in other species (Perrard et al., 2012). In particular, because of an increase in the size of emerging workers in the course of the colony cycle, wing areas of the two female castes may overlap in autumn, whereas they are clearly different in early summer. Therefore, females captured from April to June with a large wing area could be unambiguously assigned to queens, and small females captured from July to November could likewise be assigned to workers (Fig. 1B). Only such clearly identifiable individuals were used in this study (Fig. 1B; dark gray, workers; light gray, queens). For all experiments, hornets were anesthetized on crushed ice for 10 minutes before being placed in individual Plexiglas holders (see Sandoz et al., 2003, Fig. 1).

## Neuroanatomical staining

### *Whole-brain neuropil staining*

To visualize and reconstruct the hornet brain, Lucifer yellow was used as a neuropil background stain (Ai and Kanzaki, 2004; Rybak et al., 2010). The head of each hornet was fixed to the chamber with low-melting-point wax (Deiberit 502; Schöps and Dr. Böhme, Goslar, Germany), and the head capsule was opened. The brain was dissected out under phosphate-buffered saline (PBS) solution. It was then immediately transferred to 500 µl of fixative solution (4% paraformaldehyde [PFA] in PBS) containing 1 µl of 4% Lucifer yellow (Lucifer yellow CH, potassium salt, L-1177; Invitrogen, Eugene, OR) and kept for 4 days at 4°C.

### *Specific neuronal staining*

To describe the glomerular organization of the antennal lobe, antennal sensory neurons were stained anterogradely. A window was cut into the scape of each antenna, and the antennal nerves were severed with a glass electrode loaded with crystals of fluoro-ruby (tetramethylrhodamine dextran, 10,000 MW, D-1817; Invitrogen; in 2% bovine serum albumin [BSA]). The preparation was then covered with saline solution (130 mM NaCl, 6 mM KCl, 4 mM $MgCl_2$, 5 mM $CaCl_2$, 160 mM sucrose, 25 mM glucose, 10 mM HEPES, pH 6.7) and kept for 24 hours in a dark room to let the dye diffuse. On the next day, the brain was dissected out and plunged into 4% PFA solution for 24 hours at 4°C.

For visualization of projections of antennal lobe tracts (ALTs) through the protocebrum toward higher order centers, a massive dye injection in the AL was performed. The hornet's head cuticle was removed by cutting a rectangle between the antennae and the compound eyes to expose the AL neuropil.

Subsequently, a glass electrode coated with fluoro-ruby was inserted into the AL and kept in this position until dissolution of the dye crystal, allowing uptake by injured AL neurons, including projection neurons (PNs). The electrode was then dislodged from the AL, and the brain was washed with saline solution to remove extra dye. As described above, preparations were kept for 24 hours in a dark room during dye migration before brains were dissected out and fixed in 4% PFA.

### *Double labeling*

To assign AL glomeruli to one of the two main PN tracts (l-ALT, m-ALT or both), each tract was retrogradely labeled with different dyes in the same preparation. A piece of head cuticle was removed to expose the region between the ALs and the mushroom body calyces. The l-ALT was labeled by fluorescent tracer injection (dextran, Alexa Fluor 488, 10,000 MW, D-22910; Invitrogen; in 2% BSA) into the caudolateral area of the protocerebrum where the l-ALT runs between the AL and the lateral horn. The m-ALT was labeled by fluoro-ruby injection into the mediocaudal area of the protocerebrum, where the m-ALT runs between the AL and the MB. To avoid nonspecific staining, extra dye was removed after each injection by washing the brain with saline solution. After 24 hours of dye migration, the brains were dissected out and fixed in 4% PFA. To visualize olfactory and visual inputs to the MB calyces, AL projection neurons and visual output neurons were separately stained in the same preparation by mass tracer injections of Alexa Fluor into the AL and fluoro-ruby into the optic lobe (medulla and lobula).

## Brain preparations

After being removed from the fixative solution, all brains were washed three times in PBS solution (10 minutes each), dehydrated in ethanol baths following an ascending series (50%, 70%, 90%, 95%, and 3 × 100% for 10 minutes each), and clarified in methylsalicylate (Sigma-Aldrich, Steinheim, Germany) for at least 3 days at 4°C. Brains were then mounted on aluminum slides with a central hole filled with methylsalicylate and covered by thin coverslips on both sides.

## Confocal microscopy

Clarified brains were scanned from the ventral side with a laser scanning confocal microscope (LSM-700; Carl Zeis, Jena, Germany). Whole-brain optical sections were acquired at a resolution of 2.5 μm/pixels (x,y) with 3-μm intervals (z) using a water immersion objective (×10 achroplan 0.3 NA). AL optical sections were acquired at 0.52 μm/pixels (x,y) with 1-μm intervals (z) using a water immersion objective (×20 plan-apochromat 1.0 NA). Given the large size of the hornet brain, complete scans were obtained by stitching adjacent "tiles" (512 × 512 pixels) of optical sections with the tile function of the Zen software (Carl Zeiss; RRID:SCR_013672). Fluoro-ruby-labeled neurons were visualized with a 555-nm solid-state laser, whereas Lucifer yellow and Alexa Fluor were visualized with a 488-nm laser. Doubly stained neuropils were scanned sequentially to avoid emission overlap from distinct fluorescent dyes.

## 3D reconstructions and olfactory tract affiliation

Serial optical sections were saved as LSM files before adjusting brightness and contrast with ImageJ software and the Bio-formats plugin (RRID:SCR_000450). Adjusted pictures were then converted into TIFF files and imported into three-dimensional (3D) analysis software (Amira 5.4.3; FEI, Berlin, Germany; RRID:SCR_007353). Glomeruli were individually reconstructed by manual labeling in three planes (*xy*, *xz*, and *yz*) and using the Wrap function to obtain its 3D model. Larger structures, such as brain neuropils and macroglomeruli, were outlined in several stacks along one focal plane (*xy*), and the Interpolate function was used to create the 3D model.

Each reconstructed glomerulus was assigned to a glomerular cluster by closely following OSN bundles in the original scan. Because similar features such as input tract trajectories, glomerular morphologies, and output tract affiliations could be observed in different hymenopteran species, we attempted to unify olfactory tract nomenclature. Within each species, antennal sensory tracts had been previously named with numbers (T1–Tx), starting from the ventral and going to the dorsal surface of the AL (*Apis mellifera:* Suzuki, 1975; Flanagan and Mercer, 1989; Galizia et al., 1999; Kirschner et al., 2006; Nishino et al., 2009; *Camponotus* sp.: Zube et al., 2008, Nakanishi et al., 2010, Mysore et al., 2009; *Atta vollenweideri:* Kelber et al., 2010; *Cataglyphis* sp.: Stieb et al., 2011), resulting in a mismatch in tract designations between presumably homologous ones. The present study thus used a novel nomenclature, naming glomerular clusters with Roman letters ($T_A$–$T_I$), starting from the dorsal surface to the ventral surface because this arrangement better revealed similarities among different species. Among the species listed above, the hornet AL was especially compared with the honeybee and carpenter ant ALs because these species provide solid data on AL input–output connectivity. For honeybees, *A. mellifera*, we used the description of AL compartmentalization made by Kirschner et al. (2006) and Nishino et al. (2009) and our

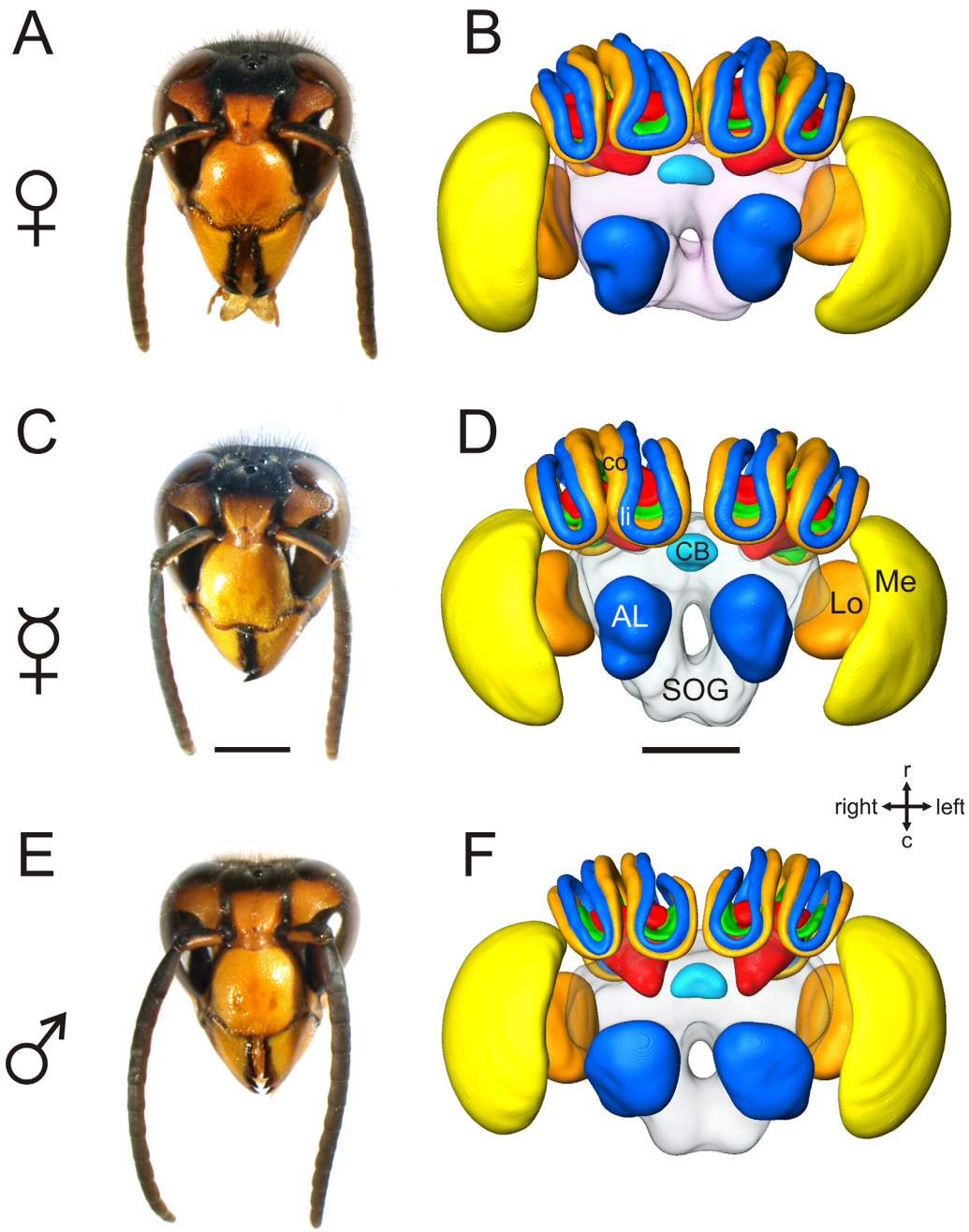


Figure 2. Head morphology and brain anatomy of the three main castes within a *V. velutina* colony. **A,C,E:** Photographs of *V. velutina* heads showing no noticeable morphological differences between queen (A) and worker heads (C) but a triangular head with longer antennae in males (E). **B,D,F:** 3D reconstructions of hornet brains. The brains of queen (B) and worker (D) do not show conspicuous differences in their organization, but slightly smaller calyces and thinner peduncles were observed in males (F). Heads and brains are shown from the ventral surfaces and are oriented following the same axis. r, Rostral; c, caudal; SOG, subesophageal ganglion; AL, antennal lobe; Me, medulla; Lo, lobula; CB, central body; li, lip; co, collar. Scale bars = 2 mm in C (applies to A,C,E); 500 μm in D (applies to B,D,F). Please click in the pdf file on D to activate the virtual content and then use the mouse to rotate the objects. Use the menu in the activated figure for further functions. [Color figure can be viewed in the online issue, which is available at wileyonlinelibrary.com.]

personal data. For carpenter ants, the descriptions by Zube et al. (2008) and Zube and Rössler (2008) for *Camponotus floridanus* and Nakanishi et al. (2010) for *C. japonicus* were used.

Spatial directions given in each figure are based on the neuraxis (Fig. 1H of Strausfeld, 2002). Consequently, rostral and caudal correspond, respectively, to anterior and posterior, according to the body axis. The

TABLE 1.
Volumes of the *V. velutina* Brain Neuropils[1]

| | Protocerebrum | Medulla | Lobula | Antennal lobe | Collar | Lip | Basal ring | Peduncle | Central body | Total |
|---|---|---|---|---|---|---|---|---|---|---|
| Queen | | | | | | | | | | |
| $\times 10^6$ μm$^3$ | 522.03 | 292.71 | 103.88 | 92.63 | 86.18 | 59.55 | 23.49 | 109.64 | 3.36 | 1.293.48 |
| Percentage | 40.36 | 22.63 | 8.03 | 7.16 | 6.66 | 4.60 | 1.82 | 8.48 | 0.26 | 100 |
| Worker | | | | | | | | | | |
| $\times 10^6$ μm$^3$ | 442.80 | 291.68 | 92.16 | 84.08 | 109.15 | 55.12 | 22.20 | 85.85 | 3.76 | 1.186.82 |
| Percentage | 37.31 | 24.58 | 7.77 | 7.08 | 9.20 | 4.64 | 1.87 | 7.23 | 0.32 | 100 |
| Male | | | | | | | | | | |
| $\times 10^6$ μm$^3$ | 428.01 | 273.23 | 94.85 | 97.46 | 58.73 | 30.83 | 15.98 | 58.17 | 3.43 | 1.060.70 |
| Percentage | 40.35 | 25.76 | 8.94 | 9.19 | 5.54 | 2.91 | 1.51 | 5.48 | 0.32 | 100 |

[1]The absolute volume (in cubic micrometers) and the relative volume (in percentage) of major brain structures are given for each caste. For multiple structures (such as the collar), the sum of all instances of this structure is given.

"frontal" surface of the brain corresponds to its most ventral region in the neuraxis.

## Data and statistical analysis

To assess caste dimorphism in the number of glomeruli, a Mann-Whitney U test was used on six reconstructed ALs from each hornet caste. Potential type I errors induced by multiple comparisons were reduced by using a Bonferroni correction ($\alpha_{corr} = 0.05/2 = 0.025$).

Glomerular volumes were calculated from 3D reconstructions in Amira 5.4.3. To overcome the problem of AL size variability in different individuals, the volume of each glomerulus was normalized with respect to the size of the AL (calculated as the sum of all glomerular volumes; Fig. 4D). To identify macroglomeruli a quantitative threshold that defines outliers according to 80% of the distribution of glomerular volumes was used:

$$V_{outlier} > V_U + k\ (V_U - V_L),$$

where $V_U$ is the upper percentile (90%) and $V_L$ the lower percentile (10%) of glomerular volume distribution. We used $k = 3$ as a conservative value that successfully categorized macroglomeruli in several hymenopteran species (Kuebler et al., 2010; Streinzer et al., 2013; Roselino et al., 2015). Thus, glomeruli whose volume was above this threshold were considered macroglomeruli.

# RESULTS

## General brain morphology

*V. velutina* males and females can be distinguished based on head and abdomen morphology, but there are no evident morphological differences between the two female castes (worker and queen; Fig. 2). Queens (Fig. 2A) are usually larger than workers (Fig. 2C), but the sizes of these two castes sometimes overlap because of the increase in the body dimensions of workers produced throughout the colony cycle. Males' heads (Fig. 2E) show a typical triangular shape that is more elongated than females' heads, with slightly more bulbous compound eyes. In addition, males' antennae are longer than those of females, with shorter scapes but 11 flagellum segments instead of 10 in females. Confocal image stacks acquired from whole-brain staining in each caste allowed 3D reconstruction of selected neuropils (Fig. 2B,D,F). No clear differences in brain structure were observed between sexes or between female castes, the different neuropils occupying similar relative volumes in all these individuals (Table 1). In particular, both male and female hornets display voluminous visual sensory structures, with 30.6% of brain volume occupied by the medulla and the lobula in the queen, 32.3% in the worker and 34.7% in the male. Likewise, the primary olfactory centers, the ALs, display only slight sexual differences in their relative sizes, with 7.2% and 7.1% of brain volume in queen and worker, respectively, and 9.2% in the male.

Hornets' mushroom bodies have a characteristic shape, with two highly voluminous calyces on each brain hemisphere and comparatively small peduncle and lobes (Fig. 2B,D,F). As in other Hymenoptera (bees, ants, etc.), the calyces are composed of three concentric and morphologically distinct areas: the collar, the lip, and the basal ring. However, in each calyx, the lips are placed more centrally compared with the collar, which bulges around the lip, resembling a double-lip from an external viewpoint (Fig. 2B,D,F). Differential mass staining of optic lobe and AL revealed that the collars are targeted by visual output neurons, whereas the lips receive only olfactory input (Fig. 3A,B). Our staining procedure revealed strong olfactory input in the hornet basal ring, but we could observe only sparse visual input in this area. Although this differential staining was not aimed at detailing visual sensory

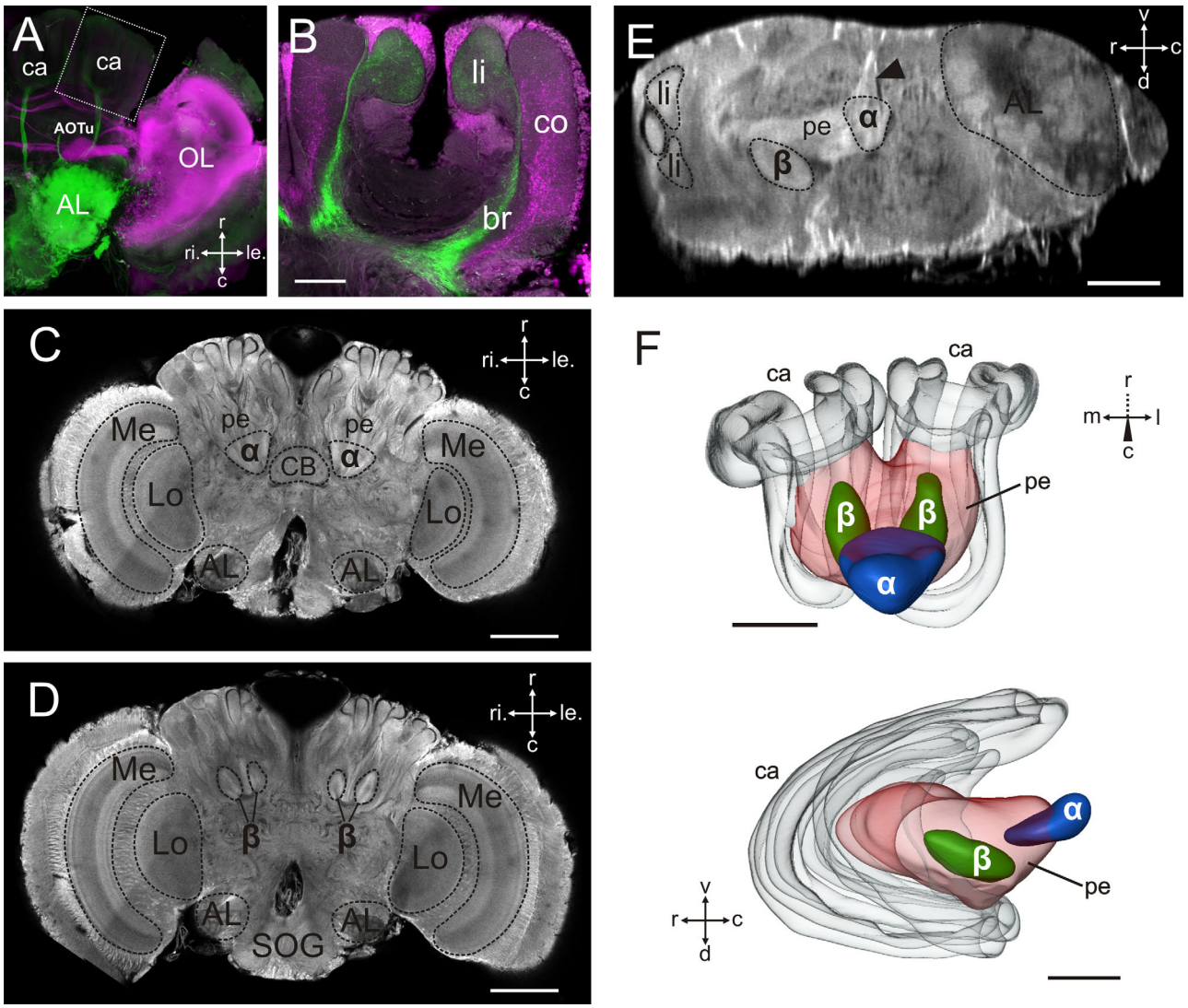


Figure 3. Mushoom body morphology in *V. velutina*. **A,B:** Frontal optical sections after mass staining in the optic lobe and in the AL with different fluorescent dyes. B: Section through the lateral mushroom body calyx (delimited in A). The collar receives visual input (magenta), whereas the lip receives olfactory input (green). **C,D:** Frontal sections through the brain at, respectively, 345 μm and 425 μm depths from the ventral surface. **E:** Sagital section of the brain. Each brain hemisphere contains a double β-lobe pointing dorsally and a single α-lobe projecting caudally, with only a fiber tract extending to the ventral surface (arrowhead). **F:** 3D model of a hornet mushroom body, showing the double β-lobe and the single α-lobe per hemisphere (left mushroom body). AL, antennal lobe; OL, optic lobe; Me, medulla; Lo, lobula; pe, peduncle; ca, calyces; li, lip; co, collar; CB, central body; r, rostral; c, caudal; v, ventral; d, dorsal; m, medial; l, lateral; ri, right; le, left. Scale bars = 80 μm in B; 400 μm in C,D; 200 μm in E,F. [Color figure can be viewed in the online issue, which is available at wileyonlinelibrary.com.]

projections in the hornet brain, it suggested an arrangement of these projections similar to that in honeybees (Mobbs, 1984; Ehmer and Gronenberg, 2002; Mota et al., 2011). In brief, a prominent visual tract, the anterior optic tract (AOT), projects into the anterior optic tubercle, whereas in the rostral part of the brain a neuronal network composed of several subtracts connects the medulla and lobula with ipsi- and contralateral MB calyces. Direct interhemispheric connections between optic lobes were observed in more dorsal layers of the brain. At this level, diffuse ipsilateral projections into the dorsal protocerebrum are also found.

Hornets' MB lobes are clearly different from those described for honeybees and ants (Mobbs, 1982, 1984; Ehmer and Gronenberg, 2004; Gronenberg, 2008). In contrast to bees' or ants' MB in which the α-lobe extends vertically to the ventral surface of the brain, the *V. velutina* α-lobe points horizontally in a caudal direction, and only a fine fiber tract attributed to MB

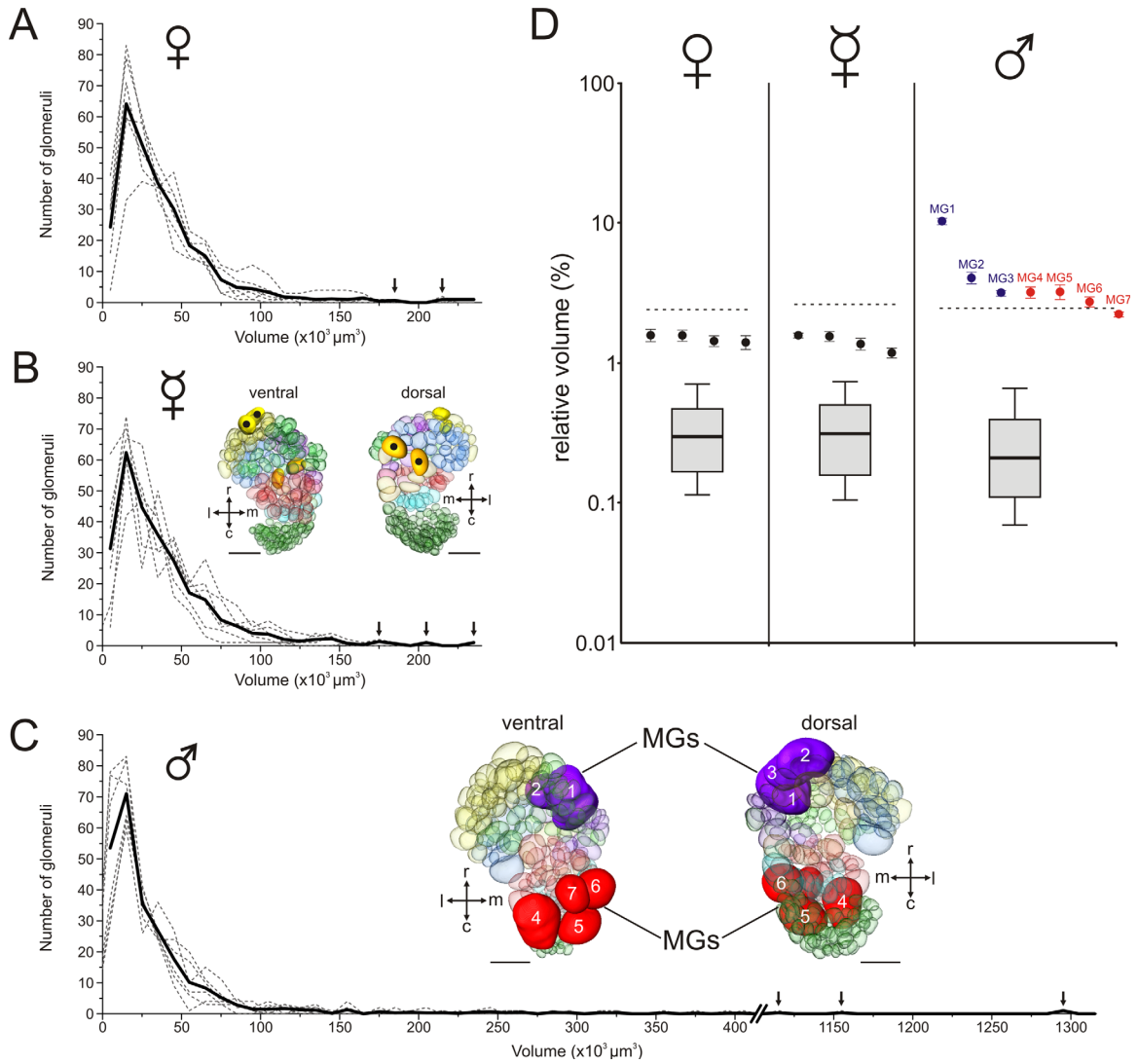


**Figure 4.** **A–C:** Glomerular volume distributions in the AL of six individuals (dotted lines) of each caste and their mean distributions (solid line). Queens (A) and workers (B) exhibit the same glomerular volume distribution. The largest glomeruli were identified at the same locations in the antennal lobes of workers and queens (black dots in B; see also Figs. (7 and 8D,E). In males (C), the upper part of the distribution extends to much greater volumes than in female castes. The AL of males contains seven hypertrophied glomeruli arranged in two clusters (MG1–7). Coloring of glomeruli relates to glomerular clusters as in Figure 7. **D:** Relative glomerular volume distribution in the three castes and positions of the largest glomeruli with regard to the statistical macroglomerulus threshold (dotted line). Dots indicate the average volume of the four (workers and queens) or seven (males) largest AL glomeruli of each caste. Only males possess glomeruli exceeding the statistical threshold. Bold lines indicate the median of glomerular volumes, boxes the first and the third quartiles (25–75%), and whiskers the 10th to 90th percentiles of the distribution. MGs, macroglomeruli; r, rostral; c, caudal; m, medial; l, lateral. Scale bars = 100 µm. [Color figure can be viewed in the online issue, which is available at wileyonlinelibrary.com.]

extrinsic neurons (see Ehmer and Hoy, 2000) extends to the ventral surface (Fig. 3C,E). Moreover, whereas honeybees' or ants' β-lobes extend horizontally toward the brain midline, the hornet β-lobe is split into two subparts, which point dorsally (Fig. 3D,E), in much the same way as previously described for the wasp *Vespula germanica* (Ehmer and Hoy, 2000).

Overall, we did not observe any clear polymorphism in the hornet brain organization except for MB calyces and peduncles, which are slightly thinner in males than in females (Fig. 2F; 21.6% of brain volume in the queen, 23% in the worker, and 15.4% in the male). The brains of the two female castes are not visually distinguishable.

## AL organization

Confocal microscopic observations after mass staining of the antennal nerve allowed the segmentation of hornets' ALs into glomerular units (n = 6 individuals

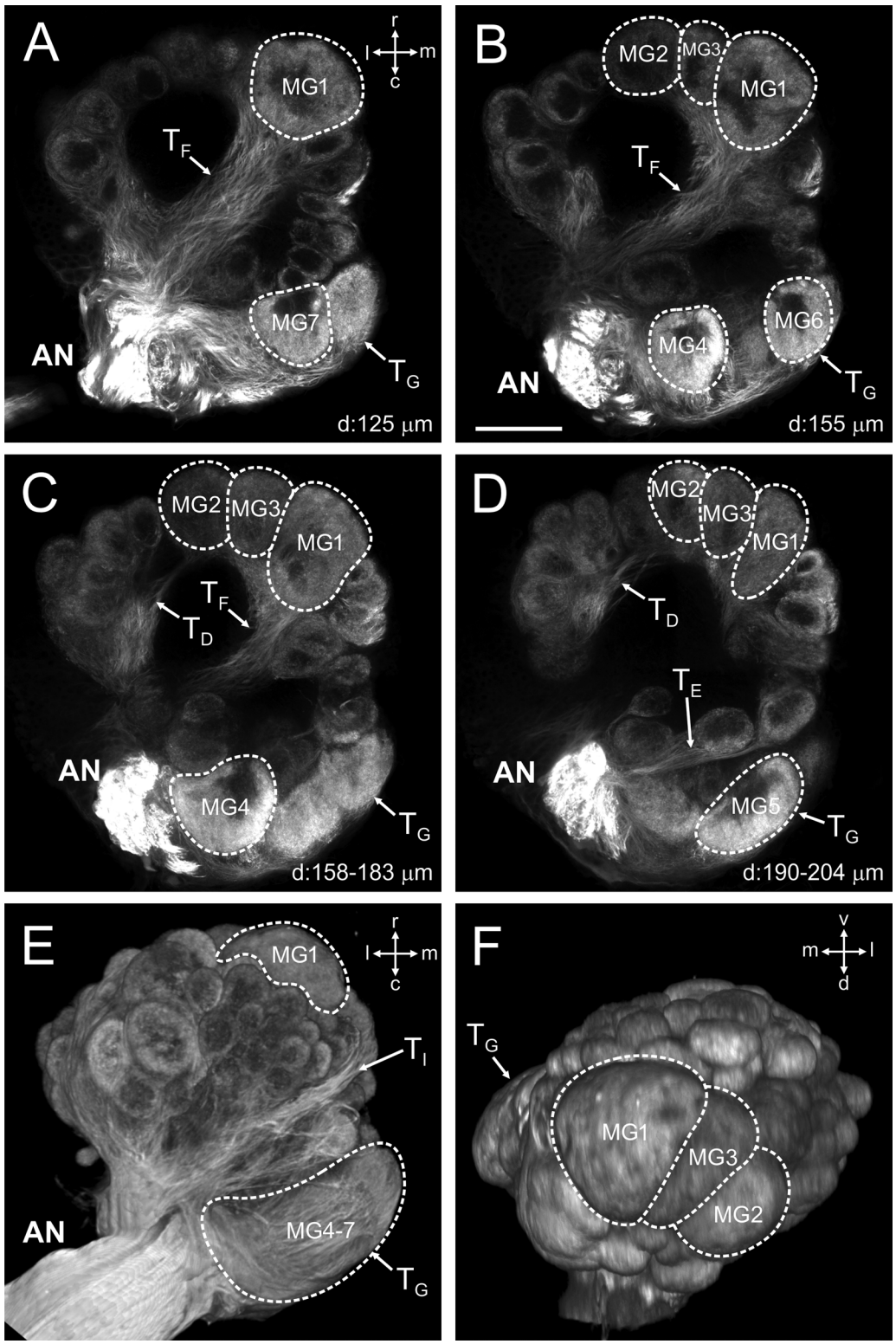


Figure 5. Macroglomeruli of the male antennal lobe. **A–D:** Confocal images (single section or z projection) at different depths from the ventral surface of a right AL in a *V. velutina* male. **E,F:** Ventral and rostral views, respectively, of a 3D volume rendering of the male AL. The macroglomeruli (dotted lines) are arranged in two clusters: the rostral cluster, receiving a thick olfactory tract through the AL, contains three macroglomeruli (MG1–3). The ventrocaudal cluster, located close to the antennal nerve entrance, contains four macroglomeruli (MG4–7). r, Rostral; c, caudal; v, ventral; d, dorsal; m, medial; l, lateral; AN, antennal nerve. Scale bar = 100 μm.

per caste). We found no difference between female castes in the number of AL glomeruli, with approximately 269 ± 9 glomeruli in queens (mean ± SD, n = 6) and 264 ± 7 glomeruli in workers (n = 6; Mann-Whitney test, U = 10, nonsignificant). We observed, however, a slight sexual dimorphism; the male AL contains 247 ± 6 glomeruli (n = 6), i.e., significantly fewer than in both female castes (Mann-Whitney test, male vs. queen, U = 1, $P < \alpha_{corr} = 0.025$; male vs. worker, U = 1, $P < \alpha_{corr} = 0.025$). From these 3D reconstructions, we measured the volumes of glomeruli in the ALs of each caste. Figure 4A–C shows individual and average distributions of glomerular volumes in queens, workers, and males (n = 6 in each group). In all castes, approximately 80% of glomerular volumes were distributed between $5 \times 10^3$ and $100 \times 10^3$ $\mu m^3$, most glomeruli displaying a volume of approximately $15 \times 10^3$ $\mu m^3$. In workers and queens, the largest glomeruli reached an absolute volume of approximately $225 \times 10^3$ $\mu m^3$. In males the distribution reached higher values, with the largest glomeruli approaching $1{,}300 \times 10^3$ $\mu m^3$. Thus, the three castes seem to share a common pattern of glomerular organization with the exception of a few substantially enlarged glomeruli in males. To determine whether these glomeruli are large enough to be termed *macroglomeruli*, we used a standard quantitative measure that defines outliers with regards to the distribution of glomerular volumes (Fig. 4D). In queens, as in workers, the four largest glomeruli are located in the most dorsal (two glomeruli) and in the ventrolateral regions (two glomeruli) of the AL (Fig. 4B, inset). They do not reach the statistical threshold and cannot be considered macroglomeruli. Similarly sized glomeruli are found at the same positions in males (see black dots, Fig. 7). By contrast, the male AL showed several enlarged glomeruli that reached the significance threshold (Figs. 4D, 5). They were grouped in two clusters, a rostral cluster containing the largest hornet macroglomerulus (MG1) and two smaller macroglomeruli (MG2, MG3), and a ventrocaudal cluster, positioned close to the antennal nerve, containing a group of four macroglomeruli. Three of them (MG4, MG5, and MG6) pass the threshold, but the fourth is marginally below the threshold. However, these four glomeruli show exactly the same OSN innervation pattern, which is much denser than that of all the other normal-sized glomeruli in this area. We thus consider this enlarged glomerulus as a possible macroglomerulus, termed *MG7*. We conclude from these observations that queens and workers have similar ALs without hypertrophied glomeruli, whereas males possess seven macroglomeruli distributed in two clusters.

## AL afferent connection pattern

We next examined the precise projection pattern of OSNs in the AL of each caste. Because close inspection of projection patterns showed that queen and worker ALs are indistinguishable, they are often described together as "female" ALs hereafter. In hornets, the antennal nerve approaches the AL laterally from the ventral side. As in other Hymenoptera, part of the antennal nerve bypasses the AL and slopes down toward the antennal mechanosensory and motor center (AMMC). OSN axons separate from this main trunk at different depths with various orientations, forming nine distinct sensory tracts, which we termed $T_A$–$T_I$, from the most dorsal to the most ventral (Fig. 6). These tracts give rise to nine clusters of glomeruli, which display distinctive morphological features. Table 2 gives an overview of glomeruli numbers and volumes for each cluster.

1. In the most dorsal part of the AL, eight glomeruli are innervated by several loose bundle tracts ($T_A$) which were particularly brightly labeled in most preparations. These glomeruli are identifiable in the three castes by their typical shapes and positional arrangements (Fig. 6M–O). They are characterized by elongated or bent shapes and receive axon terminals penetrating the entire glomerulus. Their volumes are relatively large, especially for two of them that correspond to the largest female glomeruli (black dots in Fig. 7E,F).
2. The dorsocaudal region of the AL harbors a conspicuous cluster of numerous and comparatively smaller glomeruli than in the rest of the AL, rather lightly innervated in their cortex (Fig. 6J–O). This cluster is mostly responsible for the observed variability between sexes and among individuals in the total number of AL glomeruli. Because it was not brightly stained in some preparations, the variability observed in this cluster might be due in part to difficulties in discerning all glomeruli. We counted 93 ± 7 (mean ± SD) glomeruli there in queens, 89 ± 7 glomeruli in workers, and 71 ± 5 glomeruli in males. These glomeruli receive OSN axons from the $T_B$, which originates from the ventral side and points dorsomedially (Fig. 7E,F).
3. The $T_C$ tract runs transversally through the AL, i.e., from the antennal trunk (on the lateral side) toward the dorsomedial side, determining a separation between the $T_B$ cluster and the rest of the AL (Fig. 6G,H,J–L). It sparsely innervates approximately 15 glomeruli, mostly from their caudal periphery.
4. Facing this cluster, the $T_D$ proceeds transversally through the inner dorsorostral part of the AL and

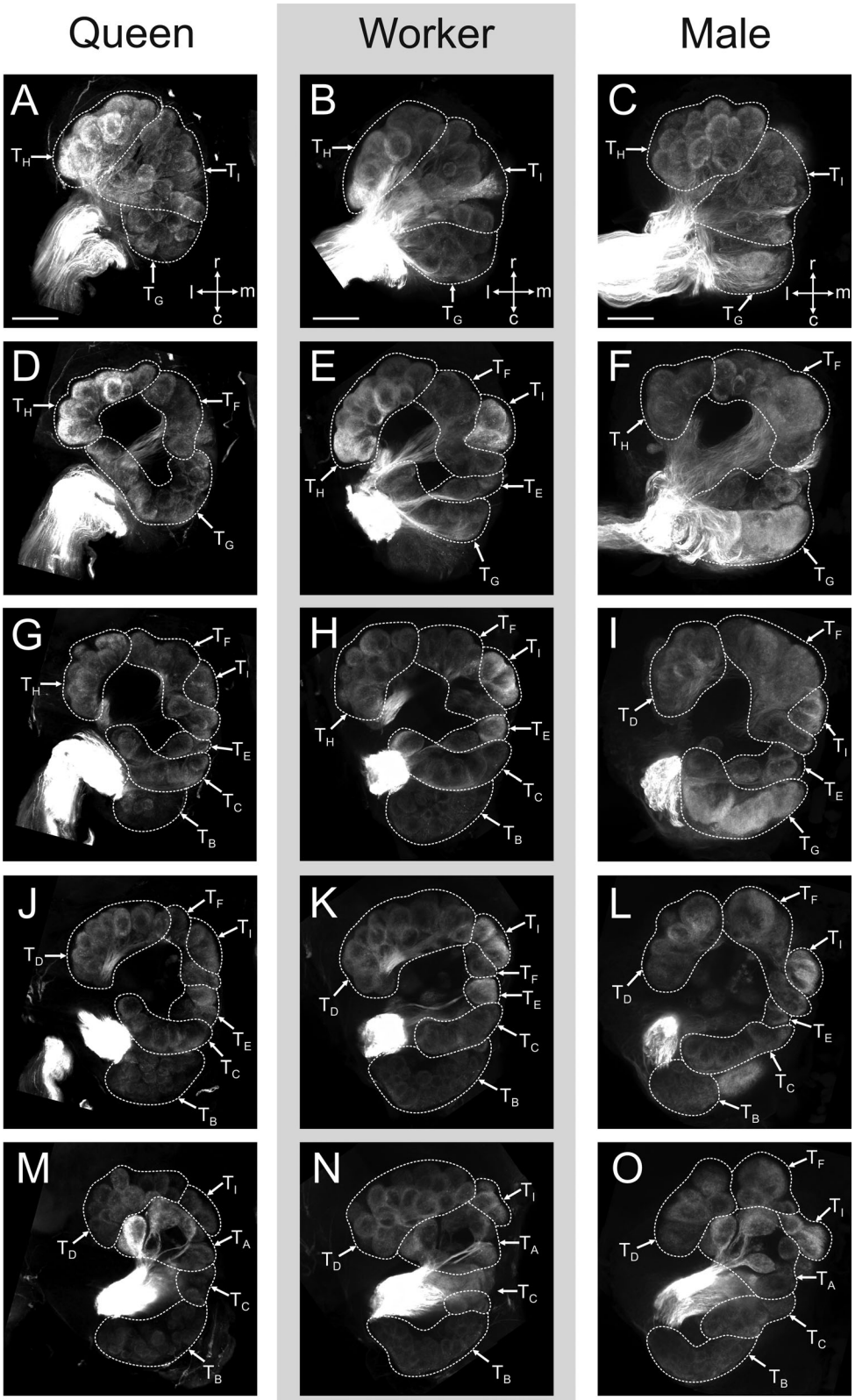


**Figure 6.** Sensory innervation of the AL of each caste. Projection views of approximately 50-μm-thick slices (~50 optical sections), starting from the ventral surface to the dorsal surface of a right AL after mass staining of the antennal nerve. The hornet AL contains nine sensory tracts ($T_A$–$T_I$) innervating distinct clusters of glomeruli. All antennal sensory tracts were observed in queens (**A,D,G,J,M**), workers (**B,E,H,K,N**), and males (**C,F,I,L,O**), but some tracts were thicker in males than in females (for instance, $T_F$ in F compared with D and E). r, Rostral; c, caudal; m, medial; l, lateral. Scale bars = 100 μm in A (applies to A,D,G,J,M); 100 μm in B (applies to B,E,H,K,N); 100 μm in C (applies to C,F,I,L,O). The complete image stack of a worker AL is provided as Supporting Information online.

densely innervates approximately 30 glomeruli in females and 25 glomeruli in males (Fig. 6I–O). We observed there a slight sexual dimorphism, with a thicker tract and relatively larger glomeruli in males, although none of them reached the macroglomerulus volume threshold (Table 2, Fig. 7E,F).

5. More ventrally, we found in both sexes a brightly labeled tract, $T_E$, that runs in the inner part of the AL, parallel to the $T_C$. This tract projects mediodorsally to only three glomeruli (Figs. 6E,G–I, 7C,D). The deepest $T_E$ glomerulus shows a bent shape similar to that of $T_A$ glomeruli and also receives axon terminals in its core region. It is, however, clearly innervated by the $T_E$ tract.
6. The $T_F$ is a thick tract that crosses the AL from the caudolateral side to the rostromedial side and innervates approximately 20 glomeruli in both males and females (Fig. 6D–F). Despite similar numbers of glomeruli between the sexes, the $T_F$ is much thicker in males. It contains numerous axons that densely project to three macroglomeruli, MG1, MG2, and MG3, forming the rostral macroglomerular cluster (Fig. 7C,D).
7. Running at the ventral surface of the AL, the $T_G$ separates from the antennal nerve and takes a mediocaudal direction. It innervates approximately 30 glomeruli mostly from the caudal periphery (Fig. 6A–F). In males, this tract is also thicker than in females and projects into four macroglomeruli close to the antennal nerve (MG4–7), forming the ventrocaudal macroglomerular cluster (Fig. 7A,B).
8. The $T_H$ spreads from the antennal nerve to the rostral surface of the AL (Fig. 6A–H). This cluster consists of approximately 30 relatively large glomeruli and contains among the largest female glomeruli (black dots, Fig. 7A,B).
9. Finally, the $T_I$ extends its axons within approximately 40 glomeruli from the lateral to the medial side of the AL, forming a cluster sided by $T_G$ and $T_H$ glomeruli (Fig. 6A–C). It innervates glomeruli on the ventral surface and then continues medially toward the dorsal side of the AL (see Fig. 6G–I).

## AL efferent pathways

Mass staining of the AL with a fluorescent dye revealed that *V. velutina* has a typical hymenopteran olfactory pathway with five output PN tracts (Fig. 8A). They seem to correspond to the three multiglomerular (ml-ALT) and two uniglomerular (l- and m-ALT) PN tracts observed in other hymenopteran species (Abel et al., 2001; Kirschner et al., 2006; Zube et al., 2008). Among the ml-ALT tracts, two leave the AL medially and

TABLE 2.
Cluster Characteristics in Hornets[1]

| | $T_A$ | $T_B$ | $T_C$ | $T_D$ | $T_E$ | $T_F$ | $T_G$ | $T_H$ | $T_I$ | Σ |
|---|---|---|---|---|---|---|---|---|---|---|
| Female | | | | | | | | | | |
| Σ Glomeruli | 8 | 90 | 15 | 29 | 3 | 22 | 33 | 29 | 37 | 266 |
| Min volume ($\times 10^3$ µm$^3$) | 51.3 | 3.3 | 11.3 | 10.5 | 58.9 | 4.6 | 8.1 | 2.5 | 10.3 | |
| Max volume ($\times 10^3$ µm$^3$) | 200.1 | 31.2 | 57.7 | 92.3 | 85.5 | 74.6 | 66.2 | 104.5 | 103.6 | |
| Mean volume ($\times 10^3$ µm$^3$) | 91.1 | 12.6 | 33.0 | 35.7 | 72.8 | 35.4 | 33.5 | 37.6 | 32.1 | |
| Output tract | m-ALT (6 of 8) | m-ALT | m-ALT | l-ALT | m-ALT (2)/ both ALTs (1) | l-ALT | l-ALT (9)/ m-ALT (24) | l-ALT | l-ALT | m-ALT (138)/ l-ALT (127) |
| Male | | | | | | | | | | |
| Σ Glomeruli | 8 | 74 | 17 | 24 | 3 | 21 | 32 | 32 | 38 | 249 |
| Min volume ($\times 10^3$ µm$^3$) | 39.4 | 2.2 | 8.5 | 6.9 | 13.7 | 1.2 | 3.72 | 5.3 | 4.1 | |
| Max volume ($\times 10^3$ µm$^3$) | 136.1 | 25.2 | 47.4 | 250.7 | 38.4 | 763.1 | 285.6 | 87.3 | 62.9 | |
| Mean volume ($\times 10^3$ µm$^3$) | 67.1 | 8.9 | 21.8 | 44.1 | 25.8 | 90.9 | 51.3 | 30.8 | 22.7 | |

[1]Number, volume, and output tract affiliation of glomeruli belonging to the nine different clusters of the antennal lobe in female and male hornets.

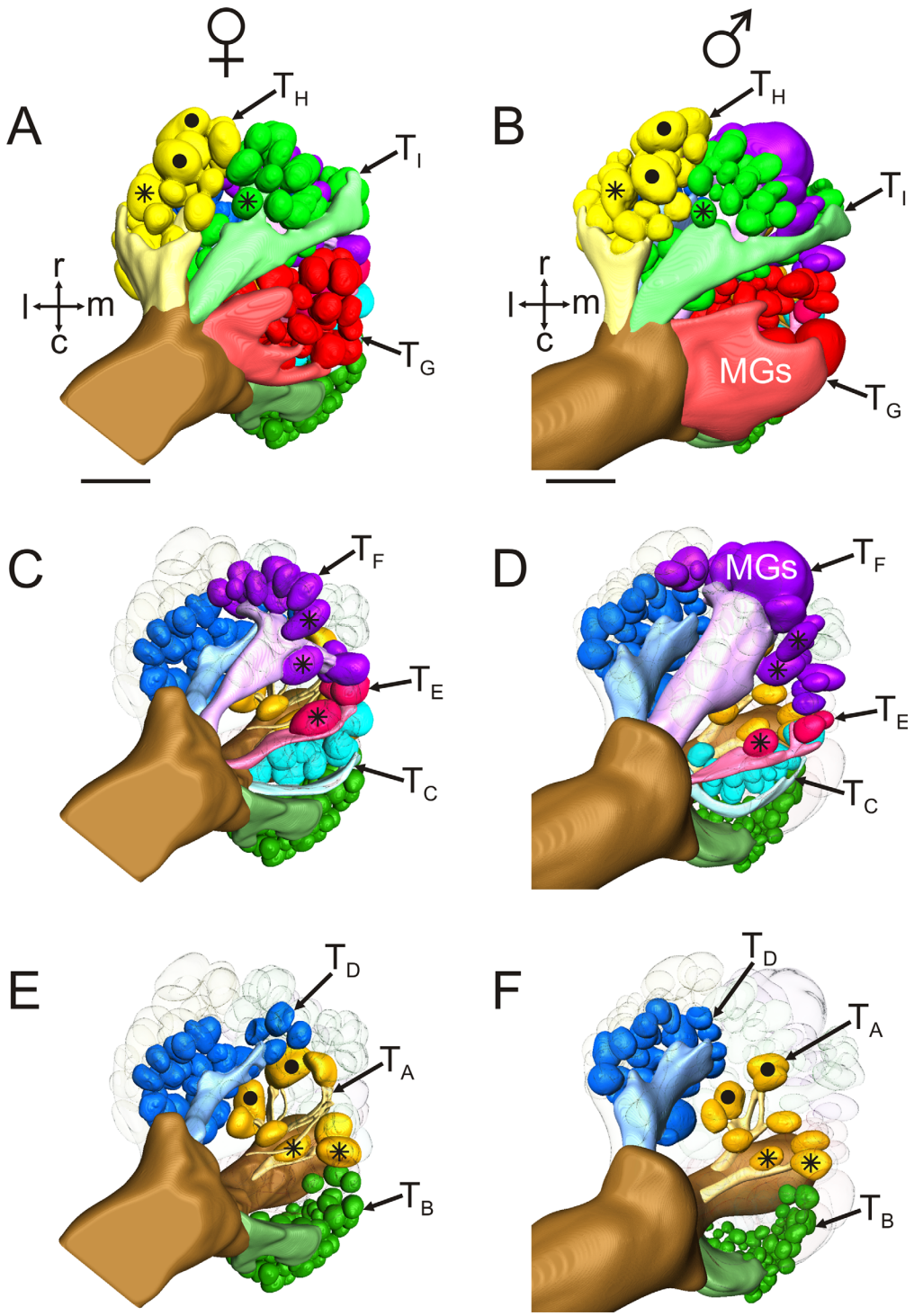


Figure 7. 3D reconstructions of the antennal lobes of *V. velutina* female (**A,C,E**) and male (**B,D,F**). The nine clusters of glomeruli and their afferent tracts ($T_A$–$T_I$) are color coded and are represented from the ventral to the dorsal surface (right AL). AL organization is highly similar in males and females, but sexually dimorphic clusters that contain macroglomeruli in males are innervated by thicker tracts ($T_F$ and $T_G$). Dots indicate the four largest glomeruli in females and their homologs in males. Asterisks indicate landmark glomeruli. r, Rostral; c, caudal; m, medial; l, lateral. Scale bars = 100 μm in A (applies to A,C,E); 100 μm in B (applies to B,D,F). [Color figure can be viewed in the online issue, which is available at wileyonlinelibrary.com.]

project transversally to the lateral protocerebrum and the LH. They contribute to a lateral network, and their characteristics are highly similar to those of the honeybee mI-ACT1 and -2 (Abel et al., 2001; Kirschner et al., 2006). A third mI-ALT tract projects rostrally and bends around the fiber tract extending from the α-lobe,

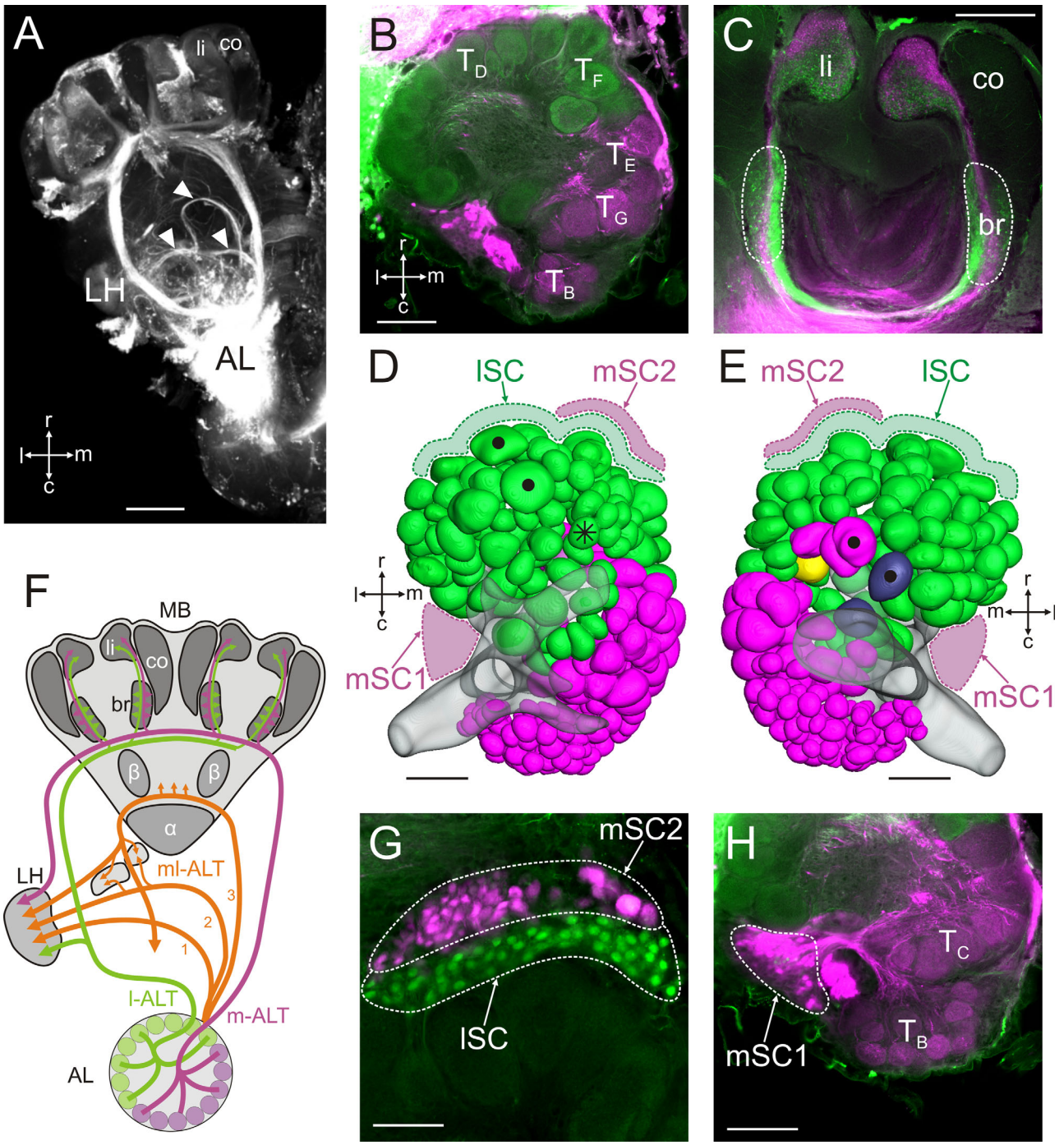


Figure 8. Efferent innervations of the AL of *V. velutina*. **A:** Projection view of an anterograde mass fill of all AL output tracts (300-µm-thick slice). Two prominent tracts (m- and l-ALT) project from the AL to the MB calyces and the LH, whereas three ml–ALTs (arrowheads) project broadly to the lateral protocerebrum and the LH. **B,C:** Optical section through the AL (B) and MB calyces (C) after differential labeling of the l-ALT (green) and m-ALT (magenta). The two output tracts arborize in segregated parts of the AL and project differentially to the lips and the basal ring of the MB calyces. **D,E:** 3D reconstruction of the *V. velutina* AL showing the affiliation of glomeruli with the two ALT output tracts (D, ventral view; E, dorsal view). Glomeruli innervated by the l-ALT (green) are in the rostroventral hemilobe of the AL, whereas m-ALT-innervated glomeruli (magenta) are located in the dorsocaudal hemilobe. Two glomeruli (dark blue) show no innervations from ALTs, whereas one glomerulus (yellow) receives processes from both m- and l-ALT. The somata of the l-ALT are spread along the rostral rim of the antennal lobe (ISC), whereas the somata of the m-ALT are distributed in a caudolateral cluster (mSC1) and a rostral cluster (mSC2). **F:** Schematic overview of the output network of the AL. **G:** Rostral somata clusters of l-ALT (ISC) and m-ALT (mSC2) neurons. **H:** Caudolateral somata cluster of the l-ALT (m-SC1). All views correspond to the right brain hemisphere. Scale bars = 200 µm in A; 100 µm in B–E,H; 50 µm in G. [Color figure can be viewed in the online issue, which is available at wileyonlinelibrary.com.]

TABLE 3.
Putative Homologies Between Glomerular Clusters in Three Well-Described Hymenopteran Species[1]

| *A. mellifera*[2] | | | *V. velutina* | | | *C. floridanus*[3] and *C. japonicus*[4] | | |
|---|---|---|---|---|---|---|---|---|
| Input tracts | Σ Glomeruli | Output tracts | Input tracts | Σ Glomeruli | Output tracts | Input tracts | Σ Glomeruli | Output tracts |
| T4 | 7 | m-ALT/5 of 7 | $T_A$ | 8 | m-ALT/6 of 8 | T7 | 6 or 10 | m-ALT/5 of 6 |
| T3b | 12 | m-ALT | $T_B$ | 90 | m-ALT | T6 | 128 or 140 | m-ALT |
| T3c | 42 | m-ALT | $T_C$ | 15 | m-ALT | T5 | 36 or 35 | m-ALT |
| | | | $T_D$ | 30 | l-ALT | T4 | 78 or 95 | l-ALT |
| T2 | 7 | l-ALT/m-ALT/both | $T_E$ | 3 | m-ALT/both | | | |
| T1 | 72 | l-ALT | $T_F$ | 20 | l-ALT | | | |
| T3a | 24 | l-ALT/m-ALT | $T_G$ | 30 | l-ALT/m-ALT | T3 | 96 or 110 | l-ALT/m-ALT |
| | | | $T_H$ | 30 | l-ALT | T2 | 56 or 45 | l-ALT |
| | | | $T_I$ | 40 | l-ALT | T1 | 34 or 35 | l-ALT |

[1]Each line contains corresponding antennal sensory tracts in honeybees (*A. mellifera*), hornets (*V. velutina*), and carpenter ants (*C. floridanus* and *C. japonicus*), with reported numbers of glomeruli and their output tract affiliations. Empty cells indicate missing tracts in the given species. Putatively homologous tracts are aligned according to the new denomination implemented in hornets, from most dorsal to most ventral.
[2]After Kirschner et al. (2006) and Nishino et al. (2009).
[3]After Zube et al. (2008) and Zube and Rössler (2008).
[4]After Nakanishi et al. (2010).

sending collaterals toward the peduncle and the lateral network. This tract ramifies in several bundles, ending in the LH and in the caudal protocerebrum. Its trajectory and projections in the protocerebrum are therefore different from those of the honeybee's ml-ACT3 (Kirschner et al., 2006). Next to these ml-ALT PNs, two prominent tracts originate from the dorsal region of the AL and run through the protocerebrum along two widely differing routes, innervating both the LH and the MB calyces. Their course resembles greatly that observed in bees (Abel et al., 2001; Kirschner et al., 2006) and ants (Zube et al., 2008). One median tract (m-ALT) projects rostrally, then follows a mediolateral route to send first collaterals to both MB calyces and then continues onward to end in the LH. The lateral tract (l-ALT) bends laterally from the exit of the AL, first sends collaterals to the LH, and then continues rostrally, eventually forming multiple branches innervating the MBs calyces. We investigated the glomerular connectivity of these tracts in the AL by differentially labeling m-ALT (magenta) and l-ALT (green) PNs (n = 2 females; Fig. 8B–H). As in honeybees and ants, both tracts arborize in different hemilobes of the AL (Fig. 8B) and project to partly segregated areas in the lips (Fig. 8B,C) and the LH (not shown). The l-ALT arborizes in ~138 glomeruli in the ventral surface and the rostral region of the AL, whereas the m-ALT arborizes in ~127 glomeruli in the dorsal and the caudal regions (Fig. 8D,E). Thus, compared with the honeybee AL, the two hemispheres of the hornet AL seem to be rotated by approximately 45° along the rostrocaudal and mediolateral axes, similarly to what has been observed in the ant *C. floridanus* (Zube et al., 2008). Somata of l-ALT neurons encircle the rostral side of the AL (lSC; Fig. 8D,E,G). By contrast, m-ALT somata are distributed mainly in two clusters, a dorsolateral cluster close to the antennal nerve (mSC1; Fig. 8D,E,H) and a rostromedial cluster located next to l-ALT somata (mSC2; Fig. 8D,E,G).

## AL input–output connectivity

To allocate glomerular clusters to either the m- or the l-ALT, we compared OSN and PN stainings of different individuals with the help of the remarkable tract architecture of the hornet AL and of landmark glomeruli (see asterisks and black dots in Figs. 7 and 8D,E). Table 2 presents the output tract affiliation of the different glomerular clusters. We observed that the $T_A$ cluster is slightly innervated by m-ALT PNs, except for two large landmark glomeruli that were not stained by either of the uniglomerular tracts. Dorsocaudal clusters, $T_B$ and $T_C$, clearly belong to the m-subsystem whereas ventrorostral clusters $T_D$, $T_F$, $T_H$, and $T_I$ clearly belong to the l-subsystem. The $T_E$ cluster is innervated by m-ALT PNs except for one glomerulus that receives processes from both m- and l-ALT neurons. Glomeruli of the $T_G$ are divided into two groups; approximately 24 glomeruli belong to the m-subsystem and nine belong to the l-subsystem.

## Common features of the hymenopteran AL

When studying the input–output connectivity of the hornet AL, we noticed conspicuous similarities to the ALs of two well-described hymenopteran species, the honeybee *A. mellifera* (Apidae) and the carpenter ants *Camponotus* sp. (Formicidae). Several glomerular clusters presented strikingly similar features in the different

TABLE 4.
Typical Features of Glomerular Clusters Across Species[1]

| | Depth | Cluster position | Uniglomerular PN output | OSN input pattern | Relative glomerular size | Glomerular features/OSN innervation |
|---|---|---|---|---|---|---|
| $T_A$ | Dorsal | Necklace arrangement | m-ALT/none | Several bundles | Large | Egg-shaped, dense innervation in both core and cortex |
| $T_B$ | Dorsal | Caudal/medial | m-ALT | From caudoventral surface | Small | Clumped glomeruli, innervation in cortex |
| $T_C$ | Relatively dorsal | Caudal/medial | m-ALT | From caudal to medial (running along TB) | Normal | Innervation in cortex, thin cortex |
| $T_D$ | Relatively dorsal | Rostral/lateral | l-ALT | Thick, inner lateral part of the AL | Normal | Innervation in cortex |
| $T_E$ | Medium | Medial | l-ALT/m-ALT/both | Through the inner medial part of the AL | Relatively large | Dense innervation in both core and cortex |
| $T_F$ | Medium | Rostral | l-ALT | Transversally through AL midline | Normal (possible sex dimorphism) | Innervation in cortex |
| $T_G$ | Relatively ventral | Medial | l-ALT/m-ALT | From caudal periphery to medial | Normal (possible sex dimorphism) | Innervation in cortex |
| $T_H$ | Ventral | Lateral | l-ALT | From lateral periphery to rostral | Relatively large | Innervation in cortex |
| $T_I$ | Ventral | Rostral | l-ALT | Caudal to rostral | Normal | Innervation in cortex |

[1]Each line gives the relative depth, the localization, and the output tract affiliation of each cluster. The fifth column indicates the projection pattern (orientation) of the olfactory sensory tract. The sixth and the seventh columns specify typical glomerular features such as relative sizes, shapes and OSN innervation types (in the whole glomerulus or only in the glomerular cortex).

species, which led us to propose a common framework for describing these ALs. Table 3 presents the putative homologies among the ALs of the three model species, and Table 4 lists the typical features defining each cluster type. The most striking observation is that all glomerular clusters found in honeybees and in ants have an equivalent cluster in hornets, whereas some clusters found in ants are not found in bees and vice versa. For observing these homologies under the best conditions, the ALs should be oriented similarly in the three species, with the antennal nerve entrance on the same axis, and the separation plane between l-ALT and m-ALT hemilobes in the same orientation across species. We detail below the clues supporting the proposed homologies:

Glomerular cluster $T_A$ is the most dorsal in hornets and presents very distinctive features, found in all three species. It contains a few large glomeruli with peculiar shapes and positional arrangements. It belongs mostly to the m-ALT subsystem, but, remarkably, two glomeruli are innervated neither by m-ALT nor by l-ALT PNs. In honeybees and carpenter ants, the most dorsal cluster (T4 in *A. mellifera,* T7 in *Camponotus*) shows the same features, which led previous authors to suggest their homology (Zube et al., 2008; Nakanishi et al., 2010). The "necklace" organization of glomeruli $T_A$-01, -03, -05, -06, and -08 in hornets greatly resembles that of glomeruli D01, D03, D05, D06, and D08 in honeybees (Fig. 9A; compare Fig. 5B of Kirschner et al., 2006). The homology is even more remarkable between the hornet $T_A$-02 glomerulus (Fig. 9A) and honeybee D02 glomerulus (see Fig. 3H,I of Kirschner et al., 2006); both are egg-shaped, positioned close to the AN, and lack any uniglomerular PN arborization.

The $T_B$ is a dorsomedial cluster, partially segregated from the main part of the AL, which flanks the antennal nerve and generally contains smaller glomeruli than the main AL, innervated by m-ALT PNs (Fig. 9A). These features clearly correspond to those of the T6 cluster of *Camponotus* workers (compare Fig. 2C of Zube et al., 2008) and are also found in the T3b of *A. mellifera*, although it contains many fewer glomeruli than in the other species (see Fig. 4A–C of Kirschner et al., 2006).

Glomeruli belonging to the $T_C$ also belong to the m-ALT subsystem. They occupy a caudomedial position within the AL of hornets and receive sensory innervations mostly from the caudal periphery of the AL. These features fit with those of the honeybee T3c and the ant T5 clusters, which have similar PNs arborization, locations, and afferent innervations (Fig. 9B; compare Fig. 3G of Kirschner et al., 2006; see also contralateral view in Fig. 2J–O of Nakanishi et al., 2010).

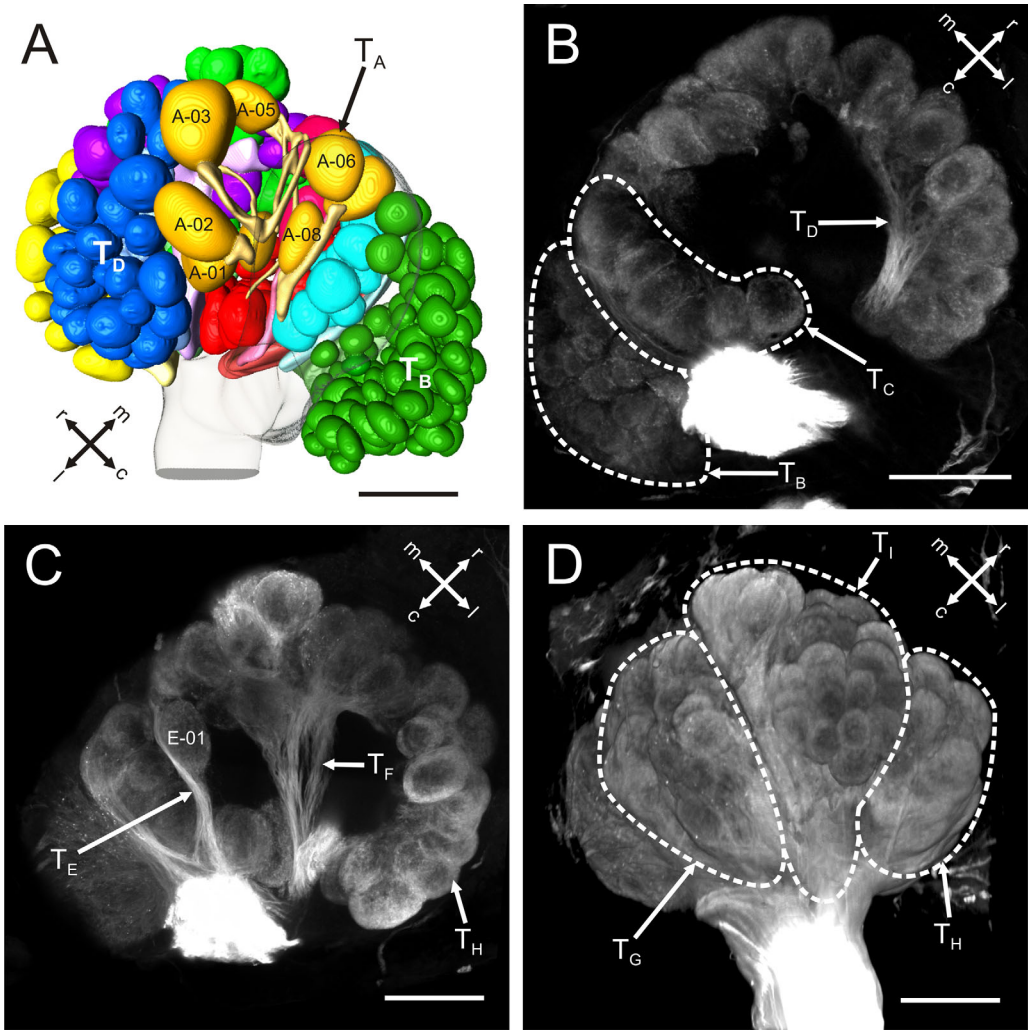


**Figure 9.** Morphological similarities between the AL of *V. velutina* and the ALs of honeybees and carpenter ants. **A:** Dorsal view of a 3D reconstruction of a *V. velutina* AL. Compare Figure 2B,C of Zube et al. (2008) and Figure 4A–C of Kirschner et al. (2006). **B:** Projection view of a 30-μm-thick slice of a left *V. velutina* AL after mass staining of the antennal nerve (depth 175–205 μm). Compare Figure 1C of Zube et al. (2008) and Figure 3G of Kirschner et al. (2006). **C:** As in B but at depth 120–150 μm. Compare Figure 3E of Kirschner et al. (2006). **D:** Ventral view of a 3D volume rendering of a left female AL. Compare Figure 3A of Zube and Rössler (2008) and Figure 2A–F of Nakanishi et al. (2010). For each picture, the antennal nerve orientation was aligned with that of bees and ants as presented in the cited studies. For comparison with previous studies, all images show a left AL. Remarkable glomerular clusters and landmark glomeruli are labeled with dotted lines and arrows. Scale bars = 100 μm. [Color figure can be viewed in the online issue, which is available at wileyonlinelibrary.com.]

The $T_D$ glomeruli belong to the l-ALT subsystem and receive axon terminals from a highly characteristic thick tract that proceeds along the inner lateral part of the AL (Fig. 9B). Similar features were observed in *Camponotus* ants with the T4 tract (compare Fig. 1C of Zube et al., 2008), but we did not find any clear correspondence in *A. mellifera*.

Conversely, two other clusters, $T_E$ and $T_F$, had clear correspondences in *A. mellifera* (with T2 and T1, respectively) but not in carpenter ants. The honeybee T2 was considered homologous to the hornet $T_E$ because in both species this sensory tract runs through the inner medial part of the AL and projects to very few glomeruli with singular shapes (Fig. 9C; compare Fig. 3E of Kirschner et al., 2006). This homology is strongly supported by the features of a landmark glomerulus. The *A. mellifera* B02 glomerulus is innervated by both l- and m-ALT PNs and receives sensory axon terminals in both its cortex and its core (see Fig. 4F,H of Nishino et al., 2009). The hornet $T_E$-01 glomerulus shows exactly the same features (Fig. 9C).

On the other hand, the putative homology between the hornet $T_F$ and the *A. mellifera* T1 is based on their similar affiliations to the l-ALT subsystem and to the conspicuous sensory tract projecting through the midline of the AL (Fig. 9C; compare Fig. 3E of Kirschner et al., 2006). In both species, it exhibits a clear sex dimorphism, being much thicker in males than in females and containing several macroglomeruli (Fig. 5B; see Fig. 5D–F of Nishino et al., 2009).

In *V. velutina* as well as in *A. mellifera* and carpenter ants, only one glomerular cluster is shared between the l- and the m-ALT subsystems, some of its glomeruli containing only l-ALT processes, others only m-ALT processes (they are termed *$T_G$*, *T3a*, and *T3*, respectively, in the three species). This cluster is located in the mediocaudal part of the AL in all species and contains glomeruli that are innervated mostly from their medial periphery (Fig. 9D; compare Fig. 1A of Zube et al., 2008; see also Fig. 3C–F of Kirschner et al., 2006).

Visually, the ventral surface of the hornet AL bears a strong resemblance to that of the carpenter ant, exhibiting similar clusters (Fig. 9D; compare Figs. 1A and 2B of Zube and Rössler, 2008). Glomeruli of the lateral surface receive sensory afferences from the $T_H$ in *V. velutina* or the T2 in *Camponotus* sp. and belong to the l-ALT. Glomeruli from the hornet $T_I$ or ant T1 cluster also belong to the l-ALT and are innervated by a sensory tract that first projects to the rostral part of the AL before sloping down dorsally (Fig. 9D; compare contralateral view Fig. 2A–F of Nakanishi et al., 2010). No equivalent of these clusters is, however, present in honeybees. All in all, these observations suggest that the hornet AL presents both honeybee and ant features.

## DISCUSSION

We studied the neuronal olfactory pathway of the hornet brain and its sex- and caste-specific adaptations. Whole-brain staining revealed that the overall organization of the *V. velutina* brain is highly similar in the two sexes and between female castes. Whereas the morphology of the hornet MBs appears distinct from that of other Hymenoptera, we found homologous structures and the same subdivision of olfactory and visual inputs (lips and collars) in the MB calyces. Our data also show that the antennal lobe of *V. velutina* consists of ~265 glomeruli distributed in nine clusters innervated by distinct antennal sensory tracts. The number of glomeruli and their volume distribution are similar between the female castes. The AL of males contains fewer glomeruli but harbors seven macroglomeruli organized in two clusters. We observed five output (PN) tracts that arborize in the AL and project to higher order centers; two prominent tracts arborize in distinct AL hemilobes and project toward partially segregated areas of MB calyces and LH, in reverse order. Three relatively smaller output tracts project through the protocerebrum toward the LH. Finally, the input–output relationships of hornet ALs display striking similarities to those of honeybees and ants, allowing a common framework for describing the olfactory pathway in these species.

### Low dimorphism in the hornet brain

Several observations that we made for hornets differ substantially from what is known in the other Hymenoptera described. First, a marked sex dimorphism within the central nervous system has been reported for many hymenopteran species and was assumed to be impelled by sexual selection (Ehmer and Gronenberg, 2004; Nishikawa, 2008; Streinzer et al., 2013; Roselino et al., 2015). The competition among males could act as a selective pressure on the sensory system for improving the localization of fertile females (Anderson and Iwasa, 1996). To assess a potential differential investment of the different sexes in particular sensory systems, the relative size of brain neuropils has been compared between males and females in several eusocial species. In these species, as in *A. mellifera* (honeybee), *Camponotus japonicus* (carpenter ant), *Atta vollenweideri* (leafcutting ant), or *Melipona scutellaris* (stingless bee), males present larger optic lobes (medulla and/or lobula) than females, suggesting sex differences in visual processing (Gronenberg and Hölldobler, 1999; Ehmer and Gronenberg, 2004; Nishikawa et al., 2008; Kuebler et al., 2010; Streinzer et al., 2013; Roselino et al., 2015). It was suggested that this sex-specific sensory adaptation is related to the importance of vision to detect and pursue fast movements of fertile females during mating flights (Ehmer and Gronenberg, 2004). Our data on the hornet *V. velutina* show that enlarged optic lobes in males are not a general feature of social Hymenoptera, as we did not find conspicuous size differences between males and females. In fact, behavioral observations in hornets in general, and *V. velutina* in particular, indicate that mating occurs on the nests or other solid substrate but not in flight (Batra 1980; Matsuura and Yamane, 1990; Monceau et al., 2014). These observations are in accordance with a less crucial role of vision in hornet males for finding their sexual partners than in other Hymenoptera. Alternatively, the hornet brain could be generally preadapted for highly demanding visual tasks (such as catching prey on the fly), so that the system is already sufficient for processing all the information relevant to mating.

Second, fewer AL glomeruli and smaller MBs in males are ubiquitous features in social Hymenoptera

and were assumed to be linked to a smaller behavioral repertoire in males (Arnold et al., 1985; Ehmer and Gronenberg, 2004; Kuebler et al., 2010; Smith et al., 2010; Streinzer et al., 2013). Typically, a lower number of glomeruli suggests a lower number of expressed olfactory receptors and can accordingly be linked to reduced olfactory discrimination abilities compared with females. In addition, smaller MBs, brain centers crucial for multimodal sensory integration, memory, and complex learning (Heisenberg, 1998; Farris, 2005; Strausfeld et al., 2009; Devaud et al., 2015), suggest lower cognitive capabilities in males. A recent comparative study underscored a less pronounced sexual dimorphism in number of glomeruli and MB size in solitary than in social bees (Streinzer et al., 2013). In contrast to males of eusocial species, which benefit from colonial altruism and leave the colony only for mating flights, males of solitary species require a higher level of behavioral plasticity, which might be responsible for such lower sex dimorphism (Stubblefield and Seger, 1994). Contrary to this general rule, we observed only ~20 (7%) fewer glomeruli in *V. velutina* males compared with females, which is clearly low compared with the ~30–40% reduction found in honeybees and carpenter ants (Arnold et al., 1985; Zube and Rössler, 2008; Nishino et al., 2009; Nakanishi et al., 2010). In the same way, the calyces and peduncle of hornet male MBs were only slightly thinner than those of females (see also Molina and O'Donnell, 2008). In hornets, males were observed to be rejected from their colony and then to perform foraging by their own means (Monceau et al., 2013, 2014). From these observations, a less pronounced sex dimorphism in the hornet brain could be attributed to a more elaborate male behavioral repertoire than in other species.

## Hornet macroglomeruli

To estimate the presence of enlarged glomeruli in the AL of *V. velutina*, we measured glomerular volumes by confocal microscopy and 3D reconstruction. We did not find any macroglomeruli in hornet females, but the male AL presented two clusters with seven strongly enlarged glomeruli. These glomerular clusters were densely innervated by OSNs, resulting in thicker $T_F$ and $T_G$ tracts in males than in females. Whereas female macroglomeruli are adaptations related to the colony life style of eusocial insects, male macroglomeruli are found throughout insects because they are involved in mating (Arnold et al., 1985; Hansson et al., 1992; Nishikawa et al., 2008; Nishino et al., 2012). In many species, such as moths or cockroaches, male-specific macroglomeruli are located in the caudal region of the AL, close to the entrance of the antennal nerve (Rospars and Chambille, 1986; Skiri et al., 2005; Nishino et al., 2012; Das and Faddamiro, 2013). In the ant *Camponotus japonicus*, two macroglomeruli at similar locations were attributed to the T3 tract and were assumed to have a sex pheromone-receptive function (Nakanishi et al., 2010). By contrast, in honeybee drones, three macroglomeruli attributed to the T1 tract are located rostrally, one of which specifically responds to the sex pheromone compound 9-ODA (Arnold et al., 1985; Sandoz, 2006; Nishino et al., 2009). Compared with other species, hornet males present numerous macroglomeruli of both types, an ant-like cluster of four ventrocaudal macroglomeruli ($T_G$), located close to the entrance of the antennal nerve and a honeybee-like cluster of three rostral macroglomeruli ($T_F$). Such sex-specific investment in several hypertrophied glomerular structures should be connected to a crucial role played by several odorants in the mating behavior of *V. velutina* males. Observation of the mating behavior of a related species, *Vespa crabro*, highlighted the existence of at least two different pheromones (Ayasse et al., 2001). Hornet females produce a long range pheromone that attracts males from long distances (Ono and Sasaki, 1987; Spiewok et al., 2006). In addition, a contact pheromone on the queen's thorax elicits copulatory behavior in males (Batra, 1980). One possibility is that one of the macroglomerulus clusters of the male hornet AL is involved in long-range detection of the sex attractant pheromone, whereas the second would process contact recognition cues such as fertility signals. More extensive data on the mating behavior of *V. velutina* and on the implicated chemical signals are needed for substantiating these hypotheses.

## A common reference for the hymenopteran AL

Despite the considerable variations observed in the number of glomeruli across hymenopteran species, previous authors have pointed out striking similarities, as well as important differences, in the organization of ant and honeybee ALs. The most remarkable similarity between these species resides in the subdivision of the AL into two hemilobes of almost equal size, separately innervated by two prominent output tracts (m- and l-ALT; Abel et al., 2001; Galizia and Rössler, 2010; Rössler and Zube, 2011). Such a dual olfactory pathway has been found in diverse taxa among Hymenoptera, except in some sawflies, suggesting its initial appearance in basal Hymenoptera (Dacks and Nighorn, 2011; Rössler and Zube 2011). In accordance with these observations, we show that Vespidae also possess such a dual pathway, which appears, as in the ant *C. floridanus,* rotated by 45° on the rostrocaudal and

mediolateral axis compared with that of the honeybee *A. mellifera*. However, we found other significant similarities among the ALs of these three species, which we attempted to integrate within a common framework (Table 3). Generally, the homologies we propose fit with and expand those proposed in an earlier work comparing bees and carpenter ants (Zube et al., 2008). We observed, based on OSN projection patterns, that the hornet AL contains nine clusters, each receiving differentially oriented branches of the antennal nerve. With similar classification rules, the AL of honeybees has been subdivided into six glomerular clusters (T1–T4, taking into account the T3a–c subdivision; Galizia et al., 1999; Kirschner et al., 2006; Nishino et al., 2009), whereas seven clusters have been identified in carpenter ants (Zube et al., 2008; Nakanishi et al., 2010). The possible homologies that we described are based mostly on neuroanatomical features related to glomerular output connectivity, OSN tract innervation patterns, cluster localizations, and average glomerular size. These features alone may not be sufficient to demonstrate these homologies unambiguously, and further comparative studies including functional data from these clusters would certainly be helpful for proving their validity. However, for some of them, available functional and neuroanatomical data already strongly support homologies across species. For instance, the $T_A$ cluster contains a few (six to 10) large glomeruli located on the most dorsal region of the AL and harbors typical whole-glomerulus OSN projections, features that fit perfectly with those of the honeybee T4 cluster (seven glomeruli; Kirschner et al., 2006; Nishino et al., 2009) and of the ant T7 cluster (6 to 10 glomeruli; Zube et al., 2008; Nakanishi et al., 2010). These glomeruli are often described as homologous to the T10 cluster of the cockroach, containing hygro-/thermosensitive neurons (Nishino et al., 2009; Watanabe et al., 2010), so homologies for this cluster may reach beyond Hymenoptera. Another strongly supported homology concerns the $T_B$ cluster. It is characterized in hornets by many small glomeruli forming a tight group slightly segregated from the main AL. This cluster has already been observed in the wasp *Polistes gallicus,* in the form of a glomerular compartment with distinct enzymatic activity compared with the main AL (Masson and Strambi, 1977). This compartment corresponds to the T6 cluster of carpenter ants (Zube et al., 2008; Nakanishi et al., 2010). This cluster is female specific in ants and bees and noticeably receives olfactory neurons housed in basiconic sensilla (Zube and Rössler, 2008; Kelber et al., 2010; Nakanishi et al., 2010; Nishikawa et al., 2012; Kropf et al., 2014). It is currently thought that these glomeruli might be involved in the processing of cuticular hydrocarbons, which are crucial for nestmate recognition in social insect colonies (Ozaki et al., 2005; Sharma et al., 2015). We recently obtained neuroanatomical and functional data suggesting a similar role in hornets, which supports the $T_B$ homology (Couto et al., in preparation).

For other clusters with less conspicuous features, homologies could be more difficult to discern and demonstrate. The present data in hornets, however, allows resolving some previous uncertainties in the comparison between honeybees and ants. Thus, the *C. floridanus* T1, T2, and T4 clusters were all suggested as possible homologous clusters to the honeybee T1 cluster (Zube et al., 2008). The honeybee T1 projects rostrally, through the middle of the AL and, in males, contains three macroglomeruli. These features are strikingly similar to those of the hornet $T_F$ (Kirschner et al., 2006; Nishino et al., 2009). In addition, we found other clusters more similar to the ants' T1, T2, and T4 tracts in the hornet AL ($T_I$, $T_H$ and $T_D$, respectively). Our current view is thus that none of the carpenter ant clusters is homologous to the T1 cluster of honeybees. Future work should strive to provide additional data allowing corroboration of the putative homologies that we have proposed. A systematic investigation of sensillar equipment (morphological types of olfactory sensilla) on the antenna, and their AL afferences in the different species (see Kropf et al., 2014; Kelber et al., 2006), along with systematic immunohistochemistry for the main neurotransmitters and neuropeptides (Masson and Strambi, 1977; Zube and Rössler, 2008; Dacks et al., 2010; Siju et al., 2014), could provide pivotal clues for testing our model.

## New insights into the evolution of the hymenopteran AL

Because the olfactory system is at the interface between the animal and its environment, it receives strong selection pressures, which induce the gain or loss of subcircuits depending on changes in the relative importance of particular chemical stimuli in the biology of the species (Ramdya and Benton, 2010). Glomerular clusters are conspicuous entities in the hymenopteran AL but it is still unclear whether different clusters are systematically involved in the detection of different odorant classes. As detailed above, for some remarkable clusters such as the $T_A$ or $T_B$, current data points in this direction. For most other clusters, however, this may not be so clear-cut because even different AL hemilobes show strongly overlapping odor response spectra (Carcaud et al., 2012; Brill et al., 2013; but see Carcaud et al., 2015). It is nevertheless possible that, within each cluster, OSNs express groups of closely

related olfactory receptor (OR) genes, as suggested by data from fruit flies. In this insect, OR genes with the highest sequence similarity tend to be expressed in OSNs targeting neighbor glomeruli, suggesting such lineage constraints on OSN projection patterns (Couto et al., 2005; Vosshall et al., 2005). This may appear through the action of specific transcription factor genes controlling OSN axon targeting (Komiyama et al., 2004; Tichy et al., 2008). Thus, the antennal sensory tract ramifications observed in Hymenoptera might be the result of genetically encoded axonal-guidance factors, which could participate in a coarse odotopic representation of odors in the AL.

The evolution of the AL is thought to entail a continuous "birth-and-death" process of ORs, inducing the budding/pruning of glomeruli within each cluster, and, eventually, of whole clusters (Ramdya and Benton, 2010). The comparative analysis of AL neuroanatomy, and the homologies that we observed, could help in retracing the evolution of the AL in Hymenoptera. At this stage, the phylogeny of Hymenoptera is not totally resolved and remains controversial (Brothers, 1999; Pilgrim et al., 2008; Heraty et al., 2011; Sharkey et al., 2012). However, according to a recent phylogeny of stinging Hymenoptera, supported by extensive genomic and transcriptomic data sets (Johnson et al., 2013), Vespidae would be more basal among aculeates than Formicidae and Apoidea, which would be sister groups. If this phylogeny is confirmed, then one could speculate that the common ancestor of Vespidae, Formicidae, and Apoidea harbored a relatively complex AL with many sensory tract subdivisions and that different secondary losses took place in Formicidae ($T_E$ and $T_F$) and Apoidea ($T_D$, $T_H$, and $T_I$). Clearly, these stimulating hypotheses can be substantiated only through the long-term study of AL neuroanatomical features and input–output relationships in a wider range of hymenopteran taxa. We note that the most strongly conserved clusters ($T_A$, $T_B$, and $T_C$) are related to the m-ALT PN tract, whereas the clusters that are related to the l-ALT output tract greatly vary among species (see Table 3). It seems remarkable that this output tract is the one that diverged more recently, probably in some basal Hymenoptera, whereas the m-ALT is the ancestral tract (Rössler and Galizia, 2010). If confirmed in other hymenopteran taxa, this could indicate that the invention of the l-ALT tract has provided Hymenoptera with a highly adaptable and plastic olfactory subsystem, potentially instrumental for their adaptation to a wide range of ecological niches and their ecological success. On the other hand, basic biological functions would be secured by the other, ancestral tract.

## ACKNOWLEDGMENTS

We thank O. Bonnard for hornet collection and K. Monceau for helpful discussion on the biology of hornets. We are indebted to J. Rybak and C. Kelber for helpful technical advice and to A.C. Roselino and F. Bastin for insightful discussion.

## CONFLICT OF INTEREST STATEMENT

All authors have confirmed that there is no identified conflict of interest, including any financial, personal, or other relationships with other people or organizations within 3 years of beginning this work that could inappropriately influence, or be perceived to influence, the work.

## ROLE OF AUTHORS

All authors had full access to all the data in the study and take responsibility for the integrity of the data and the accuracy of the data analysis. Study concept and design: AC, DT, JCS Acquisition of data: AC with help from BL. Analysis and interpretation of data: AC, JCS. Drafting of the manuscript: AC, JCS. Critical revision of the manuscript for important intellectual content: AC, DT, JCS. Obtained funding: JCS. Study supervision: JCS.

## LITERATURE CITED

Abel R, Rybak J, Menzel R. 2001. Structure and response patterns of olfactory interneurons in the honeybee, *Apis mellifera*. J Comp Neurol 437:363–383.

Ai H, Kanzaki R. 2004. Modular organization of the silkmoth antennal lobe macroglomerular complex revealed by voltage-sensitive dye imaging. J Exp Biol 207:633–644.

Andersson M, Iwasa Y. 1996. Sexual selection. Trends Ecol Evol 11:53–58.

Anton S, Homberg U. 1999. Antennal lobe structure. In: Hansson BS, editor. Insect olfaction. Heidelberg: Springer. p 97–124.

Anton S, Ignell R, Hansson BS. 2002. Developmental changes in the structure and function of the central olfactory system in gregarious and solitary desert locusts. Microsc Res Techniq 56:281–291.

Arca M, Mougel F, Guillemaud T, Dupas S, Rome Q, Perrard A, Muller F, Fossoud A, Capdevielle-Dulac C, Torres-Leguizamon M. 2015. Reconstructing the invasion and the demographic history of the yellow-legged hornet, *Vespa velutina*, in Europe. Biol Invas 17:1–15.

Arnold G, Masson C, Budharugsa S. 1985. Comparative study of the antennal lobes and their afferent pathway in the worker bee and the drone (*Apis mellifera*). Cell Tissue Res 242:593–605.

Arnold G, Budharugsa S, Masson C. 1988. Organization of the antennal lobe in the queen honey bee, *Apis mellifera* L. (Hymenoptera: Apidae). Int J Insect Morphol Embryol 17: 185–195.

Ayasse M, Paxton RJ, Tengö J. 2001. Mating behavior and chemical communication in the order hymenoptera. Annu Rev Entomol 461:31–78.

Batra SWT. 1980. Sexual behavior and pheromones of the European hornet, *Vespa crabro* germana (Hymenoptera: Vespidae). J Kansas Entomol Soc 53:461–469.

Brill MF, Rosenbaum T, Reus I, Kleineidam CJ, Nawrot MP, Rössler W. 2013. Parallel processing via a dual olfactory pathway in the honeybee. J Neurosci 33:2443–2456.

Brodmann J, Twele R, Francke W, Yi-bo L, Xi-qiang S, Ayasse M. 2009. Orchid mimics honey bee alarm pheromone in order to attract hornets for pollination. Curr Biol 19: 1368–1372.

Brothers DJ. 1999. Phylogeny and evolution of wasps, ants and bees (Hymenoptera, Chrysidoidea, Vespoidea and Apoidea). Zool Screen 28:233–250.

Bruschini C, Cervo R, Turillazzi S. 2010. Chapter nineteen—pheromones in social wasps. In: Gerald L, editor. Vitamins and hormones. New York: Academic Press. p 447–492.

Burrows M, Boeckh J, Esslen J. 1982. Physiological and morphological properties of interneurones in the deutocerebrum of male cockroaches which respond to female pheromone. J Comp Physiol A 145:447–457.

Carcaud J, Hill T, Giurfa M, Sandoz JC. 2012. Differential coding by two olfactory subsystems in the honeybee brain. J Neurophysiol 108:1106–1121.

Carcaud J, Giurfa M, Sandoz JC. 2015. Differential combinatorial coding of pheromones in two olfactory subsystems of the honey bee brain. J Neurosci 35:4157–4167.

Cardinal S, Danforth BN. 2011. The antiquity and evolutionary history of social behavior in bees. PLoS One 6:e21086.

Clifford M, Riffell J. 2013. Mixture and odorant processing in the olfactory systems of insects: a comparative perspective. J Comp Physiol A 199:911–928.

Couto A, Alenius M, Dickson BJ. 2005. Molecular, anatomical, and functional organization of the *Drosophila* olfactory system. Curr Biol 15:1535–1547.

Couto A, Monceau K, Bonnard O, Thiéry D, Sandoz JC. 2014. Olfactory attraction of the hornet *Vespa velutina* to honeybee colony odors and pheromones. PLoS One 9: e115943.

Dacks AM, Nighorn AJ. 2011. The organization of the antennal lobe correlates not only with phylogenetic relationship, but also life history: a basal hymenopteran as exemplar. Chem Senses 36:209–220.

Dacks AM, Reisenman CE, Paulk AC, Nighorn AJ. 2010. Histamine-immunoreactive local neurons in the antennal lobes of the hymenoptera. J Comp Neurol 518:2917–2933.

Das P, Fadamiro H. 2013. Species and sexual differences in antennal lobe architecture and glomerular organization in two parasitoids with different degree of host specificity, *Microplitis croceipes* and *Cotesia marginiventris*. Cell Tissue Res 352:227–235.

Devaud J-M, Papouin T, Carcaud J, Sandoz J-C, Grünewald B, Giurfa M. 2015. Neural substrate for higher-order learning in an insect: Mushroom bodies are necessary for configural discriminations. Proc Natl Acad Sci U S A 112:5854–5862.

Edwards R. 1980. Social wasps. Their biology and control. Camberley, United Kingdom: Rentokil, Ltd.

Ehmer B, Gronenberg W. 2004. Mushroom body volumes and visual interneurons in ants: comparison between sexes and castes. J Comp Neurol 469:198–213.

Ehmer B, Hoy R. 2000. Mushroom bodies of vespid wasps. J Comp Neurol 416:93–100.

Farris SM. 2005. Evolution of insect mushroom bodies: old clues, new insights. Arth Struct Dev 34:211–234.

Flanagan D, Mercer AR. 1989. An atlas and 3-D reconstruction of the antennal lobes in the worker honey bee, *Apis mellifera* L. (Hymenoptera: Apidae). Int J Insect Morphol Embryol 18:145–159.

Flögel JHL. 1878. Über den einheitlichen Bau des Gehirns in den verschiedenen Insecten-Ordnungen. Z Wiss Zool Suppl 30:556–592.

Galizia CG, Rössler W. 2010. Parallel olfactory systems in insects: anatomy and function. Annu Rev Entomol 55: 399–420.

Galizia CG, McIlwrath SL, Menzel R. 1999. A digital three-dimensional atlas of the honeybee antennal lobe based on optical sections acquired by confocal microscopy. Cell Tissue Res 295:383–394.

Groh C, Rössler W. 2008. Caste-specific postembryonic development of primary and secondary olfactory centers in the female honeybee brain. Arth Struct Dev 37:459–468.

Gronenberg W. 2008. Structure and function of ant (Hymenoptera: Formicidae) brains: strength in numbers. Myrmecol News 11:25–36.

Gronenberg W, Hölldobler B. 1999. Morphologic representation of visual and antennal information in the ant brain. J Comp Neurol 412:229–240.

Guidobaldi F, May-Concha IJ, Guerenstein PG. 2014. Morphology and physiology of the olfactory system of blood-feeding insects. J Physiol (Paris) 108:96–111.

Hansson BS, Anton S. 2000. Function and morphology of the antennal lobe: new developments. Annu Rev Entomol 45: 203–231.

Hansson B, Ljungberg H, Hallberg E, Lofstedt C. 1992. Functional specialization of olfactory glomeruli in a moth. Science 256:1313–1315.

Hansson Bill S, Stensmyr Marcus C. 2011. Evolution of insect olfaction. Neuron 72:698–711.

Hanström B. 1928. In Vergleichende Anatomie des Nervensystems der wirbellosen Tiere. Berlin: Springer-Verlag.

Heisenberg M. 1998. What do the mushroom bodies do for the insect brain? An introduction. Learn Mem 5:1–10.

Heraty J, Ronquist F, Carpenter JM, Hawks D, Schulmeister S, Dowling AP, Murray D, Munro J, Wheeler WC, Schiff N, Sharkey M. 2011. Evolution of the hymenopteran megaradiation. Mol Phylogenet Evol 60:73–88.

Hildebrand JG, Shepherd GM. 1997. Mechanisms of olfactory discrimination: converging evidence for common principles across phyla. Annu Rev Neurosci 20:595–631.

Hines HM, Hunt JH, O'Connor TK, Gillespie JJ, Cameron SA. 2007. Multigene phylogeny reveals eusociality evolved twice in vespid wasps. Proc Natl Acad Sci U S A 104:3295–3299.

Hughes WOH, Oldroyd BP, Beekman M, Ratnieks FLW. 2008. Ancestral monogamy shows kin selection is key to the evolution of eusociality. Science 320:1213–1216.

Hunt JH. 2007. The evolution of social wasps: Oxford: Oxford University Press.

Ibba I, Angioy A, Hansson B, Dekker T. 2010. Macroglomeruli for fruit odors change blend preference in *Drosophila*. Naturwissenschaften 97:1059–1066.

Ignell R. 2001. Monoamines and neuropeptides in antennal lobe interneurons of the desert locust, *Schistocerca gregaria*: an immunocytochemical study. Cell Tissue Res 306:143–156.

Ignell R, Anton S, Hansson BS. 2001. The antennal lobe of orthoptera—anatomy and evolution. Brain Behav Evol 57: 1–17.

Ikan R, Gottlieb R, Bergmann ED, Ishay J. 1969. The pheromone of the queen of the Oriental hornet, *Vespa orientalis*. J Insect Physiol 15:1709–1712.

Ishay J. 1973. Thermoregulation by social wasps: behavior and pheromones. Trans N Y Acad Sci 35:447–462.

Johnson Brian R, Borowiec Marek L, Chiu Joanna C, Lee Ernest K, Atallah J, Ward Philip S. 2013. Phylogenomics resolves evolutionary relationships among ants, bees, and wasps. Curr Biol 23:2058–2062.

Kelber C, Rössler W, Kleineidam CJ. 2006. Multiple olfactory receptor neurons and their axonal projections in the antennal lobe of the honeybee *Apis mellifera*. J Comp Neurol 496:395–405.

Kelber C, Rössler W, Roces F, Kleineidam CJ. 2009. The antennal lobes of fungus-growing ants (Attini): neuroanatomical traits and evolutionary trends. Brain Behav Evol 73:273–284.

Kelber C, Rössler W, Kleineidam CJ. 2010. Phenotypic plasticity in number of glomeruli and sensory innervation of the antennal lobe in leaf-cutting ant workers (*A. vollenweideri*). Dev Neurobiol 70:222–234.

Kirschner S, Kleineidam CJ, Zube C, Rybak J, Grünewald B, Rössler W. 2006. Dual olfactory pathway in the honeybee, *Apis mellifera*. J Comp Neurol 499:933–952.

Kleineidam C, Rössler W. 2009. Adaptations in the olfactory system of social Hymenoptera. In: Gadau J, Fewell J, Wilson E, editors. Organization of insect societies: from genome to sociocomplexity. Cambridge, MA: Harvard University Press. p 195–219.

Kleineidam CJ, Obermayer M, Halbich W, Rössler W. 2005. A macroglomerulus in the antennal lobe of leaf-cutting ant workers and its possible functional significance. Chem Senses 30:383–392.

Komiyama T, Carlson JR, Luo L. 2004. Olfactory receptor neuron axon targeting: intrinsic transcriptional control and hierarchical interactions. Nat Neurosci 7:819–825.

Kropf J, Kelber C, Bieringer K, Rössler W. 2014. Olfactory subsystems in the honeybee: sensory supply and sex specificity. Cell Tissue Res 357:583–595.

Kuebler LS, Kelber C, Kleineidam CJ. 2010. Distinct antennal lobe phenotypes in the leaf-cutting ant (*Atta vollenweideri*). J Comp Neurol 518:352–365.

Martin JP, Beyerlein A, Dacks AM, Reisenman CE, Riffell JA, Lei H, Hildebrand JG. 2011. The neurobiology of insect olfaction: sensory processing in a comparative context. Prog Neurobiol 95:427–447.

Masson C, Strambi C. 1977. Sensory antennal organization in an ant and a wasp. J Neurobiol 8:537–548.

Matsuura M, Yamane S. 1990. Biology of the vespine wasps. New York: Springer Verlag.

Mobbs PG. 1982. The brain of the honeybee *Apis mellifera*. I. The connections and spatial organization of the mushroom bodies. Philos Trans R Soc Lond B Biol Sci 298:309–354.

Mobbs PG. 1984. Neural networks in the mushroom bodies of the honeybee. J Insect Physiol 30:43–58.

Molina Y, O'Donnell S. 2008. Age, sex, and dominance-related mushroom body plasticity in the paperwasp *Mischocyttarus mastigophorus*. Dev Neurobiol 68:950–959.

Monceau K, Bonnard O, Thiéry D. 2013. Relationship between the age of *Vespa velutina* workers and their defensive behaviour established from colonies maintained in the laboratory. Insect Soc 60:437–444.

Monceau K, Bonnard O, Thiéry D. 2014. *Vespa velutina*: a new invasive predator of honeybees in Europe. J Pest Sci 87: 1–16.

Mysore K, Subramanian KA, Sarasij RC, Suresh A, Shyamala BV, VijayRaghavan K, Rodrigues V. 2009. Caste and sex specific olfactory glomerular organization and brain architecture in two sympatric ant species *Camponotus sericeus* and *Camponotus compressus* (Fabricius, 1798). Arth Struct Dev 38:485–497.

Nakanishi A, Nishino H, Watanabe H, Yokohari F, Nishikawa M. 2010. Sex-specific antennal sensory system in the ant *Camponotus japonicus*: glomerular organizations of antennal lobes. J Comp Neurol 518:2186–2201.

Nishikawa M, Nishino H, Misaka Y, Kubota M, Tsuji E, Satoji Y, Ozaki M, Yokohari F. 2008. Sexual dimorphism in the antennal lobe of the ant *Camponotus japonicus*. Zool Sci 25:195–204.

Nishikawa M, Watanabe H, Yokohari F. 2012. Higher brain centers for social tasks in worker ants, *Camponotus japonicus*. J Comp Neurol 520:1584–1598.

Nishino H, Nishikawa M, Mizunami M, Yokohari F. 2009. Functional and topographic segregation of glomeruli revealed by local staining of antennal sensory neurons in the honeybee *Apis mellifera*. J Comp Neurol 515: 161–180.

Nishino H, Iwasaki M, Kamimura I, Mizunami M. 2012. Divergent and convergent projections to the two parallel olfactory centers from two neighboring, pheromone-receptive glomeruli in the male American cockroach. J Comp Neurol 520:3428–3445.

O'Donnell S, Donlan NA, Jones TA. 2004. Mushroom body structural change is associated with division of labor in eusocial wasp workers (*Polybia aequatorialis*, Hymenoptera: Vespidae). Neurosci Lett 356:159–162.

O'Donnell S, Clifford M, Molina Y. 2011. Comparative analysis of constraints and caste differences in brain investment among social paper wasps. Proc Natl Acad Sci U S A 108:7107–7112.

O'Donnell S, Bulova SJ, DeLeon S, Khodak P, Miller S, Sulger E. 2015. Distributed cognition and social brains: reductions in mushroom body investment accompanied the origins of sociality in wasps (Hymenoptera: Vespidae). Proc R Soc Lond B Biol Sci 282:20150791.

Oi Cintia A, Van Oystaeyen A, Caliari Oliveira R, Millar Jocelyn G, Verstrepen Kevin J, van Zweden Jelle S, Wenseleers T. 2015. Dual effect of wasp queen pheromone in regulating insect sociality. Curr Biol 25:1638–1640.

Ono M, Sasaki M. 1987. Sex pheromones and their cross-activities in six Japanese sympatri species of the genus *Vespa*. Insect Soc 34:252–260.

Ono M, Igarashi T, Ohno E, Sasaki M. 1995. Unusual thermal defence by a honeybee against mass attack by hornets. Nature 377:334–336.

Ono M, Terabe H, Hori H, Sasaki M. 2003. Insect signalling: components of giant hornet alarm pheromone. Nature 424:637–638.

Ozaki M, Wada-Katsumata A, Fujikawa K, Iwasaki M, Yokohari F, Satoji Y, Nisimura T, Yamaoka R. 2005. Ant nestmate and non-nestmate discrimination by a chemosensory sensillum. Science 309:311–314.

Perrard A, Villemant C, Carpenter JM, Baylac M. 2012. Differences in caste dimorphism among three hornet species (Hymenoptera: Vespidae): forewing size, shape and allometry. J Evol Biol 25:1389–1398.

Pickett KM, Carpenter JM. 2010. Simultaneous analysis and the origin of eusociality in the Vespidae (Insecta: Hymenoptera). Arthopod Syst Phylog 68:3–33.

Pilgrim EM, Von Dohlen CD, Pitts JP. 2008. Molecular phylogenetics of Vespoidea indicate paraphyly of the superfamily and novel relationships of its component families and subfamilies. Zool Scr 37:539–560.

Ramdya P, Benton R. 2010. Evolving olfactory systems on the fly. Trends Genet 26:307–316.

Raveret Richter M. 2000. Social wasp (Hymenoptera: Vespidae) foraging behavior. Annu Rev Entomol 45:121–150.

Rome Q, Muller FJ, Touret-Alby A, Darrouzet E, Perrard A, Villemant C. 2015. Caste differentiation and seasonal changes in *Vespa velutina* (Hym.: Vespidae) colonies in its introduced range. J Appl Entomol 139:771–782.

Roselino AC, Hrncir M, da Cruz Landim C, Giurfa M, Sandoz JC. 2015. Sexual dimorphism and phenotypic plasticity in the antennal lobe of a stingless bee, *Melipona scutellaris*. J Comp Neurol 523:1461–1473.

Rospars JP. 1983. Invariance and sex-specific variations of the glomerular organization in the antennal lobes of a moth, *Mamestra brassicae*, and a butterfly, *Pieris brassicae*. J Comp Neurol 220:80–96.

Rospars JP. 1988. Structure and development of the insect antennodeutocerebral system. Int J Insect Morphol Embryol 17:243–294.

Rospars JP, Chambille I. 1986. Postembryonic growth of the antennal lobes and their identified glomeruli in the cockroach *Blaberus craniifer* burm. (Dictyoptera: Blaberidae): a morphometric study. Int J Insect Morphol Embryol 15: 393–415.

Rössler W, Brill M. 2013. Parallel processing in the honeybee olfactory pathway: structure, function, and evolution. J Comp Physiol A 199:981–996.

Rössler W, Zube C. 2011. Dual olfactory pathway in Hymenoptera: evolutionary insights from comparative studies. Arth Struct Dev 40:349–357.

Ruther J, Sieben S, Schricker B. 1998. Role of cuticular lipids in nestmate recognition of the European hornet *Vespa crabro* L. (Hymenoptera, Vespidae). Insect Soc 45:169–179.

Ruther J, Sieben S, Schricker B. 2002. Nestmate recognition in social wasps: manipulation of hydrocarbon profiles induces aggression in the European hornet. Naturwissenschaften 89:111–114.

Rybak J, Kuss A, Hans L, Zachow S, Hege H-C, Lienhard M, Singer J, Neubert K, Menzel R. 2010. The digital bee brain: integrating and managing neurons in a common 3D reference system. Front Syst Neurosci 4:30.

Sandoz JC. 2006. Odour-evoked responses to queen pheromone components and to plant odours using optical imaging in the antennal lobe of the honey bee drone *Apis mellifera* L. J Exp Biol 209:3587–3598.

Sandoz JC, Galizia CG, Menzel R. 2003. Side-specific olfactory conditioning leads to more specific odor representation between sides but not within sides in the honeybee antennal lobes. Neuroscience 120:1137–1148.

Sharkey MJ, Carpenter JM, Vilhelmsen L, Heraty J, Liljeblad J, Dowling APG, Schulmeister S, Murray D, Deans AR, Ronquist F, Krogmann L, Wheeler WC. 2012. Phylogenetic relationships among superfamilies of Hymenoptera. Cladistics 28:80–112.

Sharma Kavita R, Enzmann Brittany L, Schmidt Y, Moore D, Jones Graeme R, Parker J, Berger Shelley L, Reinberg D, Zwiebel Laurence J, Breit B, Liebig J, Ray A. 2015. Cuticular hydrocarbon pheromones for social behavior and their coding in the ant antenna. Cell Rep 12:1261–1271.

Siju KP, Reifenrath A, Scheiblich H, Neupert S, Predel R, Hansson BS, Schachtner J, Ignell R. 2014. Neuropeptides in the antennal lobe of the yellow fever mosquito, *Aedes aegypti*. J Comp Neurol 522:592–608.

Skiri HT, Rø H, Berg BG, Mustaparta H. 2005. Consistent organization of glomeruli in the antennal lobes of related species of heliothine moths. J Comp Neurol 491:367–380.

Smith AR, Seid MA, Jiménez LC, Wcislo WT. 2010. Socially induced brain development in a facultatively eusocial sweat bee *Megalopta genalis* (Halictidae). Proc R Soc Lond B Biol Sci 277:2157–2163.

Spiewok S, Schmolz E, Ruther J. 2006. Mating system of the European hornet *Vespa crabro*: male seeking strategies and evidence for the involvement of a sex pheromone. J Chem Ecol 32:2777–2788.

Spradbery JP. 1973. Wasps. An account of the biology and natural history of social and solitary wasps. Seattle: University of Washington Press.

Steinmetz I, Sieben S, Schmolz E. 2002. Chemical trails used for orientation in nest cavities by two vespine wasps, *Vespa crabro* and *Vespula vulgaris*. Insect Soc 49:354–356.

Stieb SM, Kelber C, Wehner R, Rössler W. 2011. Antennal-lobe organization in desert ants of the genus *Cataglyphis*. Brain Behav Evol 77: 136–146.

Strausfeld NJ. 2002. Organization of the honey bee mushroom body: representation of the calyx within the vertical and gamma lobes. J Comp Neurol 450:4–33.

Strausfeld NJ, Sinakevitch I, Brown SM, Farris SM. 2009. Ground plan of the insect mushroom body: Functional and evolutionary implications. J Comp Neurol 513:265–291.

Streinzer M, Kelber C, Pfabigan S, Kleineidam CJ, Spaethe J. 2013. Sexual dimorphism in the olfactory system of a solitary and a eusocial bee species. J Comp Neurol 521: 2742–2755.

Stubblefield JW, Seger J. 1994. Sexual dimorphism in the Hymenoptera. The differences between the sexes: Cambridge: Cambridge University Press.

Suzuki H. 1975. Antennal movements induced by odour and central projection of the antennal neurones in the honeybee. J Insect Physiol 21:831–847.

Tan K. 2014. Giant hornet ejecting venom to mark its territory. Abstract, 17th Congress of the IUSSI. http://hdl.handle.net/2123/11025

Tichy AL, Ray A, Carlson JR. 2008. A new *Drosophila* POU gene, *pdm3*, acts in odor receptor expression and axon targeting of olfactory neurons. J Neurosci 28:7121–7129.

Vander Meer RK, Breed MD, Espelie KE, Winston ML. 1998. Pheromone communication in social insects. Ants, wasps, bees and termites. Boulder, CO: Westview.

Veith HJ, Koeniger N, Maschwitz U. 1984. 2-Methyl-3-butene-2-ol, a major component of the alarm pheromone of the hornet *Vespa crabro*. Naturwissenschaften 71:328–329.

Viallanes H. 1887. Etude histologiques et organologiques sur les centres nerveux et les organes des sens des animaux articulés. Quatrième mémoire: le cerveau de la Guêpe (*Vespa crabro* et *V. vulgaris*). Ann Sci Nat Zool 7: 5–100.

Von Alten H. 1910. Zur Phylogenie des Hymenopterengehirns. Jen Zeitschr 46:513–590.

Vosshall LB, Wong AM, Axel R. 2000. An olfactory sensory map in the fly brain. Cell 102:147–159.

Watanabe H, Nishino H, Nishikawa M, Mizunami M, Yokohari F. 2010. Complete mapping of glomeruli based on sensory nerve branching pattern in the primary olfactory center of the cockroach *Periplaneta americana*. J Comp Neurol 518:3907–3930.

Zacharuk RY. 1980. Ultrastructure and function of insect chemosensilla. Annu Rev Entomology 25:27–47.

Zube C, Rössler W. 2008. Caste- and sex-specific adaptations within the olfactory pathway in the brain of the ant *Camponotus floridanus*. Arth Struct Dev 37:469–479.

Zube C, Kleineidam CJ, Kirschner S, Neef J, Rössler W. 2008. Organization of the olfactory pathway and odor processing in the antennal lobe of the ant *Camponotus floridanus*. J Comp Neurol 506:425–441.